Fast Atom Bombardment

10

Learning Objectives

- Ablating action of energetic particles on surfaces
- Secondary ion formation by impact of primary ions and neutrals
- Desorption of ions from condensed phase into the gas phase
- Moderating effect of a liquid matrix
- FAB and LSIMS – general properties and applications
- Air- and moisture-sensitive samples
- Related desorption/ionization techniques based on particle impact

Particles impinging on surfaces with kinetic energies in the range of kilo- or even megaelectronvolts cause the ejection of neutrals along with a small fraction of ions from the surface material exposed to their bombardment. The impacting particles are either atoms, molecules, or clusters and it is generally irrelevant whether these are neutrals or ions – what matters is their high kinetic energy. Such ions bombarding the surface are called *primary ions*, those originating from and released by the surface material are referred to as *secondary ions*.

10.1 Brief Historical Sketch

Secondary ion mass spectrometry (SIMS) employing the sputtering effect of a beam of impacting ions was first applied to bulk, inorganic materials. As outlined in the reviews of Benninghoven [1] and Honig [2, 3] the technique had only sparsely been used and mentioned until the end of the 1960s (Chap. 15). Later, attempts were made to also use SIMS for the analysis of organic solids [4, 5]. Prior to this, biomacromolecules had only been analyzed by ^{252}*Californium* (^{252}Cf) *plasma desorption* (PD) time-of-flight (TOF) mass spectrometry (Sect. 10.7). Another

J.H. Gross, *Mass Spectrometry*, DOI 10.1007/978-3-319-54398-7_10

technique called *molecular beam solid analysis* (MBSA) which employed impacting energetic neutrals had also been available at that time but was not widely used in laboratories, at least not under its original name [6, 7]. Unfortunately, SIMS conditions caused electrostatic charging of organic surfaces upon ion impact, and thus this led to a disadvantageous interfering with ion source potentials. Employing a beam of energetic neutral atoms in analogy to the MBSA technique eliminated such problems and promoted further developments of this promising method [8, 9] – the technique was later named *fast atom bombardment* (FAB) [8–10].

It turned out that ions of intact molecular species could be generated even in case of highly polar compounds that definitely were no candidates for electron ionization (EI, Chaps. 5 and 6) or chemical ionization (CI, Chap. 7). Early FAB-MS suffered from rapid radiolytic decomposition of the samples caused by irradiation and from the comparatively harsh conditions of desorption/ionization. The use of a *liquid matrix* in which the analyte was dissolved meant a major breakthrough [11, 12]. Today one would refer to this as "matrix-assisted fast atom bombardment" [13, 14]. FAB-MS soon became the major competitor of field desorption (Chap. 8). It turned out that the properties of the liquid matrix are of key importance for the resulting FAB spectra [15–17]. Due to some electric conductivity of the matrix, primary ions could now again be employed successfully [18–21].

When primary ions instead of neutrals are used to provide the energy for secondary ion ejection from the liquid matrix, the technique is termed *liquid secondary ion mass spectrometry* (LSIMS, Table 10.1). Next to FAB and LSIMS, "inorganic" SIMS has tremendously developed to become a versatile method for surface analysis and more recently for molecular imaging applications (Sect. 15.6).

Table 10.1 Desorption/ionization methods employing impact of energetic particles

Method	Acronym	Principle
Secondary ion mass spectrometry	SIMS	Sputtering and ionization by a beam of ions impacting on solids with keV-energies [1–3]
Plasma desorption	PD-MS	Desorption/ionization of biomolecules by impact of single megaelectronvolt nuclear fission fragments [22–24]
Molecular beam solid analysis	MBSA	Ion formation by impact of neutral molecules with keV-energies on organic solids [6, 7]
Fast atom bombardment	FAB	Desorption/ionization from solids and most importantly liquid matrices by a beam of neutral atoms with keV-energies [8, 9]
Liquid secondary ion mass spectrometry	LSIMS	Desorption/ionization from samples dissolved in a liquid matrix by a beam of ions with keV-energies [18, 19]
Massive cluster impact	MCI	Generation of secondary ions by bombardment with massive clusters of up to 10^8 u [25]

Any energetic particle will do
Apart from kinetic energy and momentum, the characteristics of the primary particles is of lower importance [26] because only minor differences are observed between FAB and LSIMS spectra. In the following, because of the otherwise small differences between the two methods, reference to FAB will be meant to include LSIMS.

10.2 Molecular Beam Solid Analysis

Molecular beam solid analysis (MBSA) was the first technique to use a beam of energetic neutrals to achieve sputtering – or ablation as this is called nowadays – and ionization of solid samples [6, 7]. The MBSA technique employed argon and krypton for primary beam generation. The noble gas was first ionized in a primary ion source, the ions were accelerated by a high voltage of several kV and then neutralized by transmitting the primary ion beam through a charge transfer cell with the neutral gas of the same species. While losing their charge, the primary particles did not suffer a notable change in kinetic energy (Fig. 10.1 and cf. Sect. 10.3). The neutral beam then hit the analyte material on a target in the analytical ion source where analyte got ablated and – at least some small fraction of it – becoming ionized. The ions were then extracted for mass analysis in a magnetic sector analyzer.

Analysis of inorganic salts by MBSA Let's take a look at the positive-ion secondary ion mass spectrum of a piece of filter paper after deposition and evaporation of an equimolar solution of LiF, NaCl, RbBr, and CsI (0.01 M each) as shown below (Fig. 10.2). Argon was used to generate the primary beam. By MBSA, the alkali cations are efficiently desorbed into the gas phase along with some other ions generated from the paper, e.g., $C^{+\bullet}$, *m*/*z* 12. Also note the characteristic isotopic patterns caused by the pairs of $^{6}Li/^{7}Li$ and $^{85}Rb/^{87}Rb$ in contrast to the monoisotopic ions of ^{23}Na and ^{133}Cs. Similarly, MBSA had also been applied successfully to metals and minerals.

MBSA application to organic compounds Organic molecules have also been successfully analyzed by MBSA. The sample needed to be of low volatility and had to have a molecular weight of less than about 500 u. MBSA spectra of diphenylamine and *N*-(2-nitrophenyl-)aniline show prominent molecular ion peaks of the respective compound (Fig. 10.3), i.e., *m*/*z* 169 corresponding to $[C_{12}H_{11}N]^{+\bullet}$ and *m*/*z* 214 due to $[C_{12}H_{10}N_2O_2]^{+\bullet}$ [7]. The peak at *m*/*z* 168 in b) corresponds to a loss of NO_2 from the molecular ion. Overall, the degree of fragmentation appears comparable to that observed in chemical ionization.

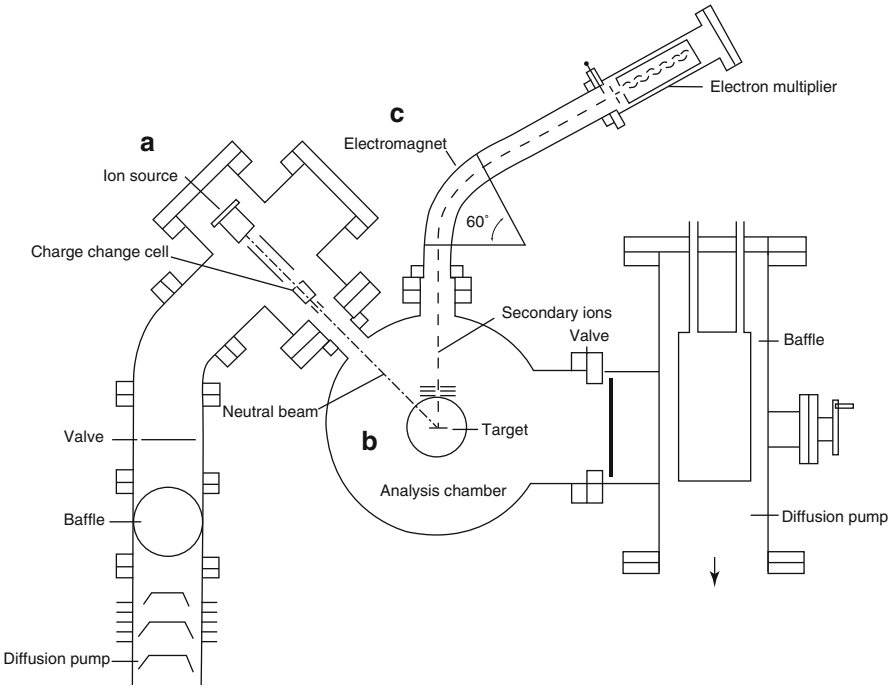

Fig. 10.1 MBSA instrument. The noble gas is ionized in the primary ion source (**a**) and ions of the gas are accelerated and guided through a charge transfer cell. The neutral beam hits a target in the analytical ion source (**b**) where sample material gets sputtered and ionized. Ions are extracted for mass analysis into a magnetic sector analyzer (**c**) (Reproduced from Ref. [7] by permission. © Wiley, 1982)

10.3 Ion Sources for FAB and LSIMS

10.3.1 FAB Ion Sources

An ion source for FAB can be constructed by suitable modification of an EI ion source (Sect. 5.1). Most importantly, the source needs to be modified to give free access to the fast atom beam. The electron-emitting filament and the ion source heaters are switched off during FAB operation (Fig. 10.4). The FAB gas is introduced via a needle valve into the lower part of the *FAB gun* mounted above the ion source. From there, it effuses into the ionization chamber of the FAB gun and into the ion source housing. The *saddle field gun* [27] is the most common type of FAB gun, delivering a primary particle flux of some 10^{10} s^{-1} mm^{-2} [28, 29]. The gas is ionized and the ions are accelerated by a high voltage (4–8 kV) and focused onto the sample [8, 10, 14, 30]. Neutralization of the energetic noble gas ions is effected by charge transfer with incoming neutrals (Sects. 7.4 and 9.17.4). The kinetic energy of the atoms is mostly conserved during charge transfer, and thus the

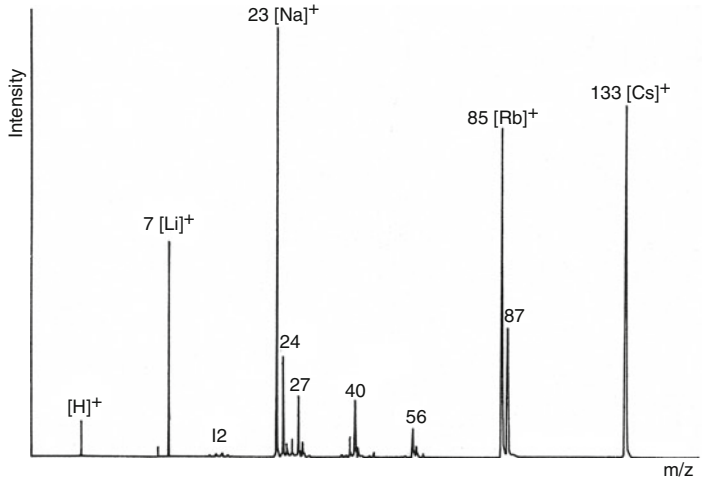

Fig. 10.2 Application of MBSA to inorganic analysis demonstrated by the positive secondary ion mass spectrum resulting after evaporation of an equimolar solution of LiF, NaCl, RbBr, and CsI (0.01 M each) on filter paper. Note the isotopic patterns by the pairs of $^{6}Li/^{7}Li$ and $^{85}Rb/^{87}Rb$ (Reproduced from Ref. [7] by permission. © Wiley, 1982)

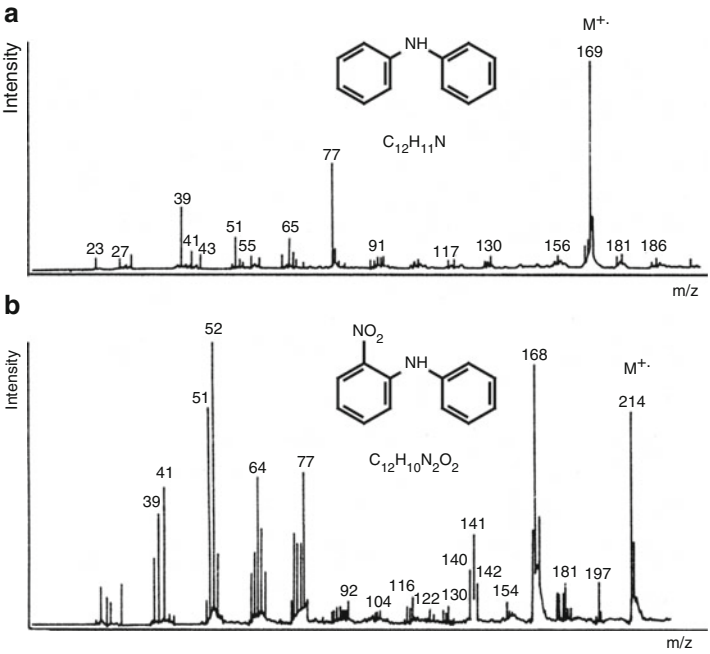

Fig. 10.3 MBSA spectra of (**a**) diphenylamine and (**b**) *N*-(2-nitrophenyl-)aniline. Both spectra show prominent molecular ion peaks of the compounds, i.e., in (**a**) *m/z* 169 corresponding to $[C_{12}H_{11}N]^{+\bullet}$ and in (**b**) *m/z* 214 due to $[C_{12}H_{10}N_2O_2]^{+\bullet}$ (Adapted from Ref. [7] by permission. © Wiley, 1982)

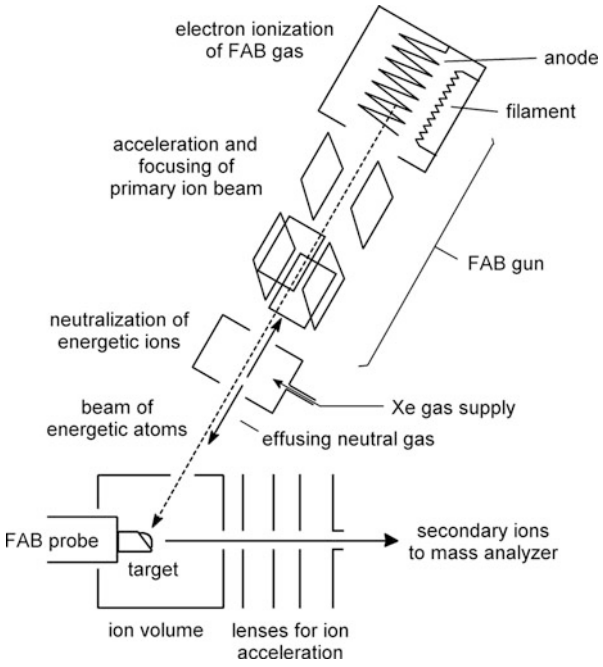

Fig. 10.4 Schematic of a FAB ion source and a FAB gun

neutrals hit the exposed surface with high kinetic energy. The fact that neutralization is not quantitative is not an issue as long electrostatic charging of the sample is avoided [26]. Ion guns for the generation of energetic noble gas ions can therefore be employed without disadvantage [31]. Xenon is preferred over argon and neon as FAB gas [32, 33], because it transfers a higher momentum when impacting onto the surface at equal kinetic energy (Fig. 10.5).

Similarity of FAB and MBSA
Having read the description on the design and operation of the FAB gun and the FAB ion source, you will have noticed the close similarities of MBSA and early FAB instrumentation. The Barber group developed the technique to full maturity and introduced the liquid matrix as the decisive detail enabling the analysis of high-mass, polar, and even ionic analytes by FAB-MS.

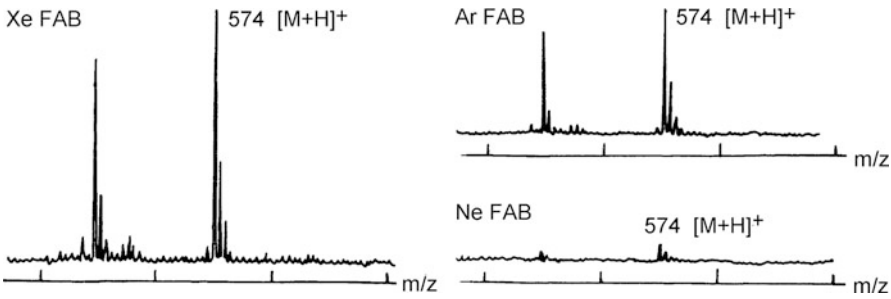

Fig. 10.5 Comparison of the efficiency of xenon, argon, and neon FAB gas for the FAB mass spectrum of the small peptide Met-enkephalin. The intensities are in scale (Reproduced from Ref. [32] by permission. © Elsevier Science, 1983)

Load to the vacuum system

Effusing FAB gas and evaporating matrix present an additional load to the high vacuum pump of the ion source housing, necessitating sufficient pumping speed (300–500 l s^{-1}) for stable operation. In contrast to EI and CI ion sources, FAB ion sources are operated without heating to reduce evaporation of the matrix and thermal stress of the analyte. Accordingly, the ion source is contaminated with matrix. Often, ion sources are constructed as EI/CI/FAB combination ion sources. After FAB measurements, it is therefore recommended to heat and pump the ion source overnight prior to EI or CI operation.

10.3.2 LSIMS Ion Sources

As mentioned before, primary ions can also be employed to provide the energy for secondary ion emission when organic compounds are admixed to a liquid matrix [18–20]. Cs^+ ions are preferentially used in organic *liquid secondary ion mass spectrometry* (LSIMS). The Cs^+ ions are produced by *thermal ionization* (Sect. 15.2) from a surface coated with cesium alumina silicate or other cesium salts [18]. Temperatures of about 1000°C are necessary to generate a sufficient flow of primary ions, and thus precautions must be taken to shield the LSIMS ion source from that heat. The Cs^+ ions are extracted, accelerated, and focused onto the target as usual by electrostatic lenses [34–36]. An advantage of Cs^+ ion guns is that the beam energy can be more widely varied, e.g., in the 5–25 keV range, in order to adjust for optimized secondary ion emission [36]. Especially with high-mass analytes, Cs^+ ion guns generally yield superior ion emission as compared to Xe FAB [26]. In order to further increase the momentum of the primary ions, gold

negative atomic ions [37], as well as molecular and massive cluster ions (Sect. 10.8) have been used as primary ions.

10.3.3 FAB Probes

The analyte, either solid or admixed to some liquid matrix, is introduced into the FAB ion source by means of a probe bearing a sample holder or *FAB target*. The FAB target usually is a stainless steel or copper tip that exposes the analyte at some angle (30–60°) to the fast atom beam. The target can have a plane or more specifically cup-shaped surface to hold a 1–3 µl drop of matrix/analyte mixture (Fig. 10.6). Normally, the target is maintained at ion source temperature, i.e., only slightly above ambient temperature. Heating or – more importantly – cooling can be provided with special FAB probes only (Sect. 10.6.5).

10.3.4 Sample Preparation for FAB and LSIMS

Despite the fact that the small amount of matrix on the tip of the probe employed to introduce the sample into the ion source, sample preparation for FAB or LSIMS is quite simple.

Sample preparation usually works best when the analyte can be dissolved in a suitable solvent as to produce a solution of about 1 mg ml^{-1} which is then admixed to the matrix. This can directly be performed on the tip by placing 1–2 µl of analyte solution on top of a 1–3 µl drop of matrix.

The probe is inserted into the vacuum lock after most of the solvent has evaporated, which generally takes just half a minute. Residual solvent is quickly removed during roughing just before the lock opens towards the high vacuum of the ion source housing.

Alternatively, some tiny crystals of the analyte may directly be dissolved in the matrix. To do so, the tip of a fine pin or needle is first dipped into the analyte and

Fig. 10.6 FAB probe of a JEOL JMS-700 magnetic sector instrument (*left*). The probe tip with a drop of glycerol placed onto the exchangeable stainless steel FAB target (*right*)

then transferred and dipped into the matrix. Gentle stirring of the matrix drop helps to dissipate and dissolve the analyte. This may analogously be applied to high-boiling liquid or viscous samples.

10.4 Ion Formation in FAB and LSIMS

10.4.1 Ion Formation from Inorganic Samples

The energy provided by the impacting primary particle causes a collision cascade in the upper atomic or molecular layers of the sample. Within 30–60 ps, a cylindrical expansion is effected in the sample along the path of penetration [19]. Not all of this energy is dissipated and absorbed in deeper sample layers. A portion is directed toward the surface, where it effects ejection of material into the vacuum (Fig. 10.7) [21]. Due to the primary particle flux employed, this mode of operation corresponds to the *dynamic SIMS* mode as described in Sect. 15.6 in more detail.

In case of a bulk inorganic salt such as cesium iodide, Cs^+ and I^- ions are heading away from the surface [38]. Those ions having the suitable polarity are attracted by the extraction/acceleration voltage, those of opposite charge sign are pushed back onto the surface. Held together by strong interionic forces, ionic clusters may desorb as such or dissociate in the liquid–gas interface layer due to their internal energy content.

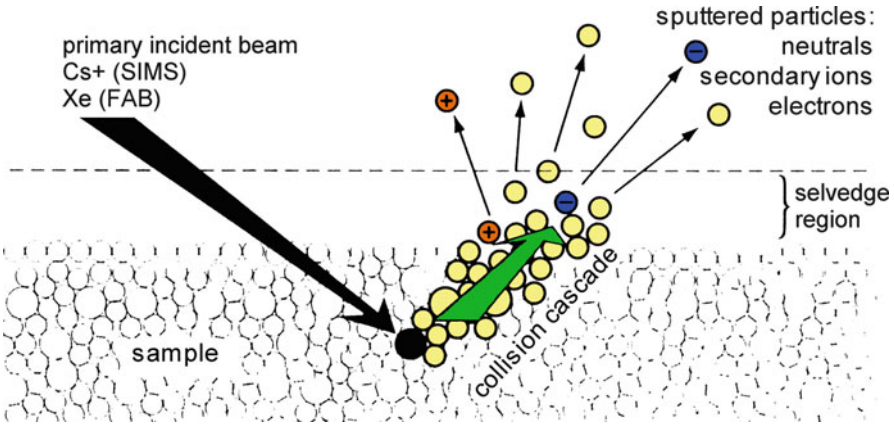

Fig. 10.7 Simple illustration of an instantaneous collision cascade generated as a result of primary particle impact in desorption/ionization mass spectrometry (Adapted from Ref. [21] by permission. © John Wiley & Sons, 1995)

FAB/SIMS of inorganic compounds Bombardment of cesium iodide or gold delivers cluster ion series which are useful for mass calibration of the instrument over a wide range. CsI works equally well in positive- and negative-ion mode to yield $[(CsI)_nCs]^+$ and $[(CsI)_nI]^-$ cluster ions, respectively (Fig. 10.8). Starting from $n = 0$, $[(CsI)_nCs]^+$ cluster ions have been observed up to m/z 90,000 [38]. Larger $[(CsI)_nCs]^+$ cluster ions dissociate to yield smaller ones: $[(CsI)_nCs]^+ \rightarrow [(CsI)_{n-x}Cs]^+ + (CsI)_x$ [39]. Gold produces a negative $Au_n^{-\bullet}$ cluster ion series up to about m/z 10,000 [40].

Monoisotopic standards
Cs, I, and Au are all monoisotopic. This presents an advantage in that it assures the peak top to exactly represent the theoretical isotopic mass of the respective cluster ion, independent of its m/z ratio or actual resolution (Sects. 3.2 and 3.4). CsI, KI, and other alkali salts that provide more narrow-spaced cluster ion series can alternatively be employed as saturated solutions in glycerol [41–43].

10.4.2 Ion Formation from Organic Samples

According to Todd "it is a common feature of FAB and LSIMS that they defy any generally acceptable mechanistic description" [44]. Unlike EI or CI, where ions are generated from gaseous molecules, desorption/ionization techniques involve a state transition from liquid or solid to the gas phase *and* ionization of neutral molecules. Nonetheless, reviews dealing with the processes of desorption and ion formation

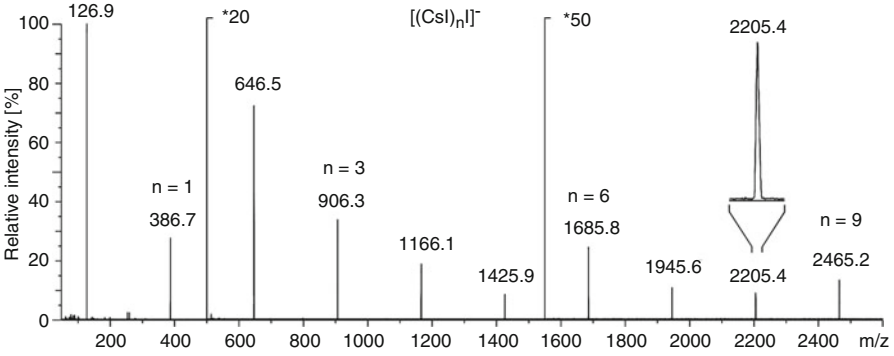

Fig. 10.8 Negative-ion FAB spectrum of solid CsI. The monoisotopic $[(CsI)_nI]^-$ cluster ion series (cf. expanded view of m/z 2205.4) is well suited for calibrating a wide mass range

under FAB and LSIMS conditions offer some insight [19–21]. Basically, there are two major concepts, the *chemical ionization model* on one side [44–48], and the *precursor model* on the other [48–52].

The *chemical ionization model* of FAB assumes the formation of analyte ions to occur in the liquid–gas interface layer some micrometers above the liquid matrix. In this space, a plasma state similar to the reagent gas plasma in chemical ionization can exist powered by the quasi-continuous supply of energy from a stream of impacting primary particles. The present reactive species may undergo numerous bimolecular reactions, the most interesting of them being the protonation of analyte molecules to yield $[M + H]^+$ ions. Plasma conditions could also explain the observation of $M^{+\bullet}$ and $M^{-\bullet}$ radical ions as formed in case of low-polarity analytes. Here, the primary particle beam serves to sputter material from the liquid surface and to subsequently ionize neutrals by particle impact (cf. EI, Sect 5.1) in the gas phase. Matrix molecules, preferably ionized for statistical reasons, may then act as reagent ions to effect CI of the gaseous analyte. Striking arguments for this model are the facts that ion formation largely depends on the presence of gaseous matrix [45, 46], and that FAB spectra of volatile analytes are closely similar to the corresponding CI spectra [48].

The *precursor model* of FAB applies well to ionic analytes and samples that are easily converted to ionic species within the liquid matrix, e.g., by protonation or deprotonation or due to cationization. Those *preformed ions* would simply have to be desorbed into the gas phase (Fig. 10.9). The promoting effect of decreasing pH (added acid) on $[M + H]^+$ ion yield of porphyrins and other analytes supports the precursor ion model [51, 52]. The relative intensities of $[M + H]^+$ ions in FAB spectra of aliphatic amine mixtures also do not depend to the partial pressure of the amines in the gas phase, but are sensitive on the acidity of the matrix [53]. Furthermore, incomplete desolvation of preformed ions nicely explains the observation of matrix (Ma) adducts such as $[M + Ma + H]^+$ ions. The precursor model bears some similarities to ion evaporation in field desorption (Sect. 8.6).

Many neutrals, few ions

It has been estimated that a single impact causes the eruption of about 10^3 secondary neutrals, but yields only 0.02–1.5 ions [42, 44, 53, 54]. The ions are then heading away from the surface in a *supersonic expansion* at speeds of about 1000 m s^{-1} [19, 42].

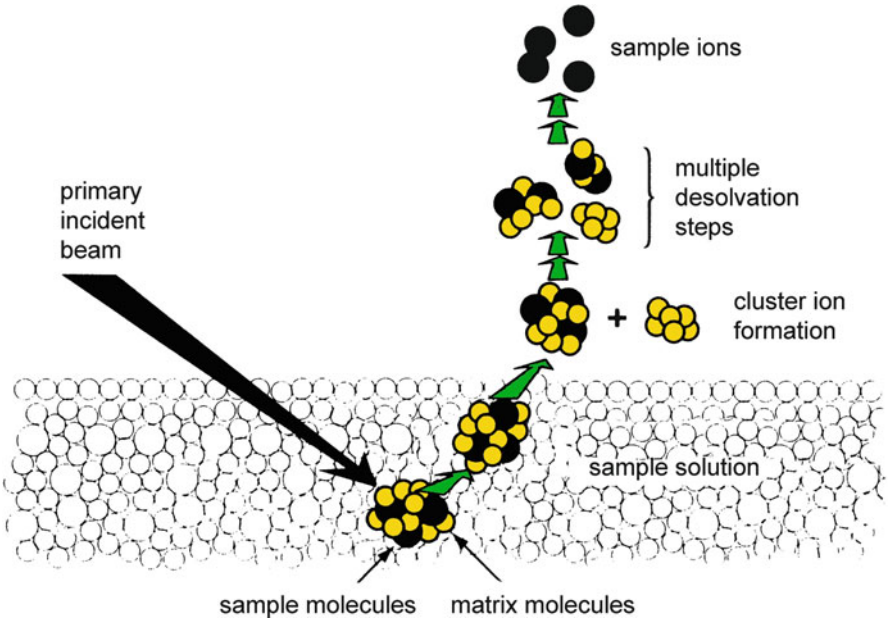

Fig. 10.9 In LSIMS and FAB, sample–matrix cluster ion formation and desolvation processes occur on a longer time scale (Adapted from Ref. [21] by permission. © John Wiley & Sons, 1995)

10.5 Liquid Matrices for FAB and LSIMS

10.5.1 The Role of the Liquid Matrix

Soon after the first use of a glycerol matrix, the importance of a liquid matrix for FAB was recognized [14]. Other organic solvents of low volatility were explored in order to obtain better spectra. The tasks of the matrix are numerous [19, 20, 33, 55, 56]:

- It has to absorb the primary energy.
- By solvation it helps to overcome intermolecular forces between analyte molecules or ions.
- The liquid matrix provides a continuously refreshing and long-lasting supply of analyte.
- It assists analyte ion formation, e.g., by yielding proton donating/accepting or electron donating/accepting species upon bombardment.

Nowadays, numerous matrices are in use (Table 10.2). Several reviews on FAB matrices in general [16, 17, 55–57] and papers on special matrices [15, 58, 59] have been published.

Table 10.2 Matrices for FAB-MS

Matrix	Uses	References
3-Nitrobenzyl alcohol (NBA)	Highly versatile, general purpose, medium polarity, first trial	[60–62]
2-Nitrophenyl octylether (NPOE)	General purpose, aprotic matrix	[15, 60]
Glycerol	Polar matrix, good for internal calibration on matrix signals	
Thioglycerol	Peptides, reductive character	[13]
"Magic bullet" (eutectic 5:1 mixture of dithiothreitol/dithioerythritol)	Peptides, small proteins, reductive character	[63]
Triethanolamine (TEA)	Basic, highly polar matrix, good for $[M - H]^-$ production	[15]
Di-, tri-, and tetraethyleneglycols	Polar, less volatile than glycerol	[13, 15]
Liquid paraffin	Aprotic, inert	[64–66]
Sulfolane	Effective solvent, rather volatile	[67, 68]
Concentrated sulfuric acid	Highly acidic, good for internal calibration on matrix signals	[69]

Scheme 10.1

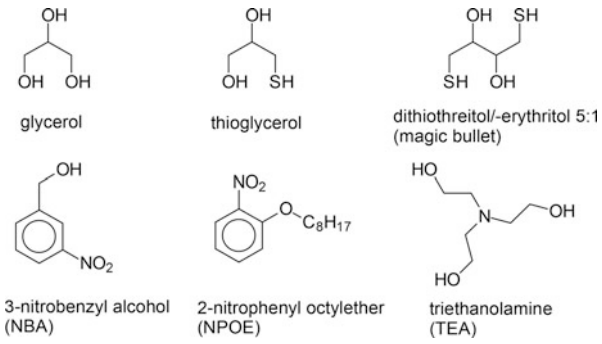

An ideal FAB matrix should fulfill the following criteria [19, 20, 33, 55, 56] (Scheme 10.1):

- The analyte should be soluble in the matrix. Otherwise, addition of co-solvents, e.g., dimethylformamide (DMF), dimethylsulfoxide (DMSO), or other additives [70, 71] can become necessary.
- Only low-vapor pressure solvents can be easily used as a matrix in FAB. In principle, volatile solvents can be employed, provided a stable surface can be obtained on the time scale of recording a mass spectrum.
- The viscosity of the solvent must be low enough to ensure the diffusion of the solutes to the surface [72].
- Ions from the matrix itself should be as unobtrusive as possible in the resulting FAB spectrum.
- The matrix itself has to be chemically inert. However, specific ion formation reactions promoting secondary ion yield are advantageous.

Note
A great advantage of FAB is that the matrix can be perfectly adapted to the analyte's requirements. On the other hand, using the wrong matrix can result in complete suppression of analytically useful signals.

10.5.2 FAB Matrix Spectra: General Characteristics

FAB matrix spectra are generally characterized by a series of matrix (Ma) cluster ions accompanied by some more abundant fragment ions in the lower *m*/*z* range. In positive-ion FAB, $[Ma_n + H]^+$ cluster ions predominate, while $[Ma_n - H]^-$ cluster ions are preferably formed in negative-ion FAB (Fig. 10.10). The principal ion series may be accompanied by $[Ma_n + \text{alkali}]^+$ ions and some fragments of minor intensity, e.g., $[Ma_n + H - H_2O]^+$. The fragment ions detected below the $[Ma + H]^+$ ion, which normally also gives rise to the base peak, are almost the same as

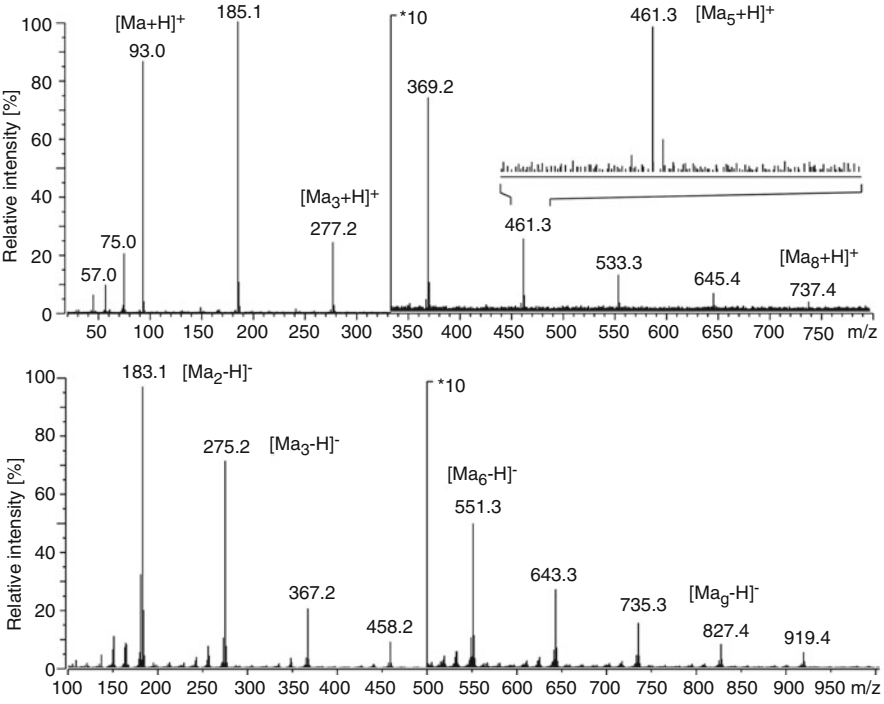

Fig. 10.10 FAB spectra of neat glycerol, $M_r = 92$ u. (**a**) Positive ions (for the positive-ion CI spectrum of glycerol, see Sect. 7.2.5); (**b**) negative ions. The expanded view in (**a**) shows the "peak at every *m*/*z*-character" of FAB spectra

observed in the positive-ion CI mass spectrum of the respective matrix compound [42].

In addition to the prominent cluster ions, radiolytic decomposition of the matrix generates an enormous number of different ions, radicals, and cluster ions resulting thereof [73, 74]. Despite being of minor intensity, they contribute to the "peak at every *m*/*z*-character" of FAB spectra, i.e., there is significant *chemical noise* (Sects. 1.6 and 5.2.4) [75, 76]. During elongated measurements, the changes of the matrix spectrum due to increasing radiolytic decay are clearly visible [73]. High kinetic energy of impacting primary particles combined with reduced particle flux seem to diminish destructive effects of irradiation [77].

10.5.3 Unwanted Reactions in FAB-MS

The conditions of the FAB process also promote unwanted reactions between analyte and matrix. Even though such processes are not relevant in the majority of FAB measurements, one should be aware of them. Besides addition or condensation reactions with matrix fragment ions [78, 79], reduction [80–83] and dehalogenation [84, 85] of the analyte represent the more prominent side-reactions in FAB. Electron transfer causing the reduction of otherwise doubly charged ions have also been observed [43].

10.6 Applications of FAB-MS

10.6.1 FAB-MS of Analytes of Low to Medium Polarity

The FAB plasma provides conditions that allow to ionize molecules by either loss or addition of an electron to form positive molecular ions, $M^{+\bullet}$ [48, 86], or negative molecular ions, $M^{-\bullet}$, respectively. Alternatively, protonation or deprotonation may result in $[M + H]^+$ or $[M - H]^-$ ions. Their occurrence is determined by the respective basicity or acidity of analyte and matrix. Cationization, preferably with alkali metal ions, is also frequently observed. Often, $[M + H]^+$ ions are accompanied by $[M + Na]^+$ and $[M + K]^+$ ions as already noted with FD-MS (Sect. 8.6). Furthermore, the joint occurrence of both $M^{+\bullet}$ and $[M + H]^+$ ions of one compound is not unusual [48]. In case of simple aromatic amines, for example, the peak intensity ratio $M^{+\bullet}/[M + H]^+$ increases as the ionization energy of the substrate decreases, whereas 4-substituted benzophenones show preferential formation of $[M + H]^+$ ions, regardless of the nature of the substituents [87]. It can be assumed that protonation is initiated when the benzophenone carbonyl groups form hydrogen bonds with the matrix.

Exchangeable protons can be replaced by alkali ions without affecting the charge state of a molecule. Thus, $[M - H_n + \text{alkali}_{n+1}]^+$ and $[M - H_n + \text{alkali}_{n-1}]^-$ ions can

also be observed if one or more acidic hydrogens are easily exchanged [5, 18, 43, 71, 88, 89]. The addition of cation exchange resins or crown ethers may help to reduce alkali ion contaminations [90]. Double protonation to yield $[M + 2H]^{2+}$ ions or double cationization [43] are only observed with high-mass analytes [91, 92] and otherwise remain an exception in FAB. Which of the above processes will most effectively contribute to the total ion yield strongly depends on the actual analyte–matrix pair.

FAB spectrum of tetramesitylporphyrin The positive-ion FAB spectrum of tetramesitylporphyrin, $C_{56}H_{54}N_4$, in NBA matrix exhibits $M^{+\bullet}$ and $[M + H]^+$ ions (Fig. 10.11) [93]. The presence of both species can be recognized by comparison of experimental and calculated M + 1 ion intensity. This difference is due to about 20% $[M + H]^+$ ion formation. The diffuse groups of signals around *m/z* 900 reveal the formation of some adduct ions with the matrix, e.g., $[M + Ma + H - H_2O]^+$ at *m/z* 918.

FAB spectra of polyethyleneglycols Polyethyleneglycols (PEGs) of average molecular weights up to about 2,000 u are well soluble in NBA. Resulting from their flexible polyether chain, $H(OCH_2CH_2)_nOH$, PEGs are easily cationized by loose complexation with Na^+ or K^+ ions. Traces of alkali salts are sufficient to prefer $[M + alkali]^+$ over $[M + H]^+$ ions. The positive-ion FAB spectrum of PEG 600 in NBA nicely shows the molecular weight distribution of the oligomer (Fig. 10.12). The peaks belonging to the same series are displayed at 44 u distance.

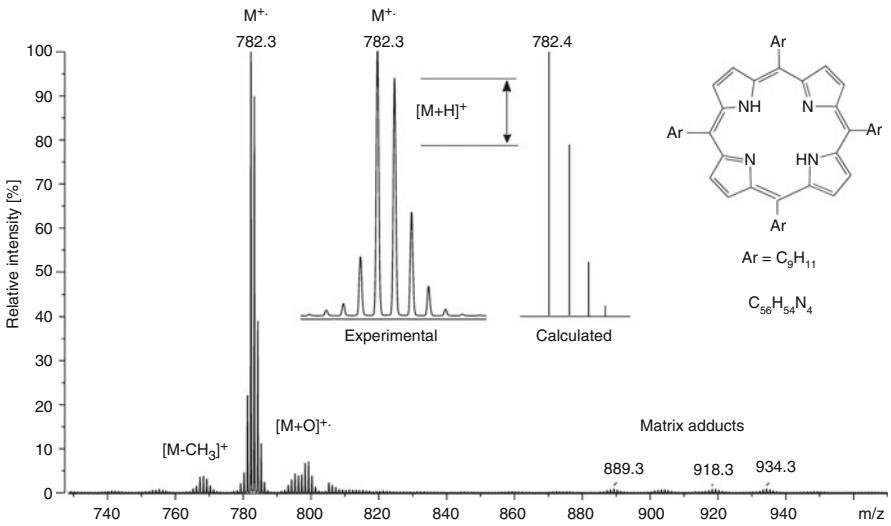

Fig. 10.11 Partial positive-ion FAB spectrum of a tetramesitylporphyrin in NBA matrix. Comparison of the experimental and calculated isotopic patterns reveals the presence of $M^{+\bullet}$ and $[M + H]^+$ ions (Adapted from Ref. [93] by permission. © IM Publications, 1997)

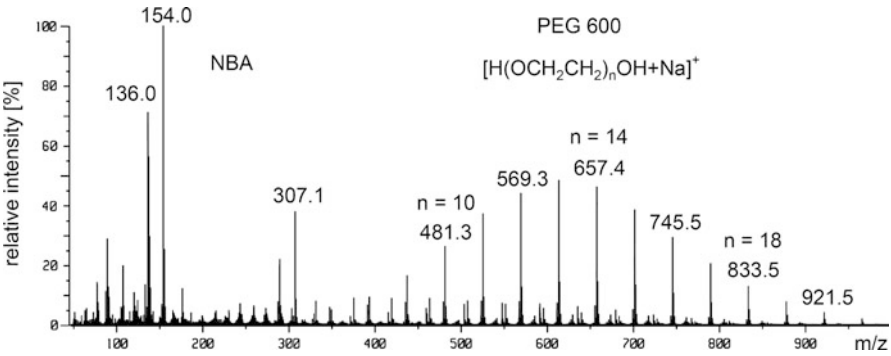

Fig. 10.12 Positive-ion FAB spectrum of polyethyleneglycol of average molecular weight 600 u (PEG 600) in NBA matrix

10.6.2 FAB-MS of Ionic Analytes

FAB is well suited for the analysis of ionic analytes. In positive-ion mode, the spectrum is usually dominated by the cationic species, C^+, which is accompanied by cluster ions of the general composition $[C_n + A_{n-1}]^+$. Thus, the distance between these signals corresponds to the complete salt [CA], i.e., yields its "molecular" weight. This behavior is perfectly analogous to FD (Sect. 8.6). In negative-ion FAB, the anion A^- will cause the base peak of the spectrum, and accordingly, cluster ions of the type $[C_{n-1} + A_n]^-$ are formed in addition. Consequently, both cation and anion are usually identified from the same FAB spectrum, irrespective of the chosen polarity. Nonetheless, it is common practice to select the polarity of the more interesting ion for the measurement.

Provided the salt is sufficiently soluble in the matrix, the signals normally exhibit high intensity as compared to those of the matrix. This result is consistent with the model of preformed ions in solution that only need to be desorbed into the gas phase.

Organic salts analysis by positive-ion FAB-MS The positive-ion FAB spectrum of an immonium perchlorate, $[C_{14}H_{16}N]^+$ ClO_4^- [94], dissolved in NBA is dominated by the immonium ion (C^+) at *m/z* 198 (Fig. 10.13). The perchlorate counterion can well be identified from the cluster ions $[2C + A]^+$, *m/z* 495, and $[3C + 2A]^+$, *m/z* 792. The signal at *m/z* 495 is expanded to demonstrate that chlorine is readily recognized from its isotopic pattern (Sect. 3.2.4).

Organic salts analysis by negative-ion FAB-MS The Bunte salt $[CH_3(CH_2)_{15}S\text{-}SO_3]^-$ Na^+ yields a very useful negative-ion FAB spectrum from NBA matrix (Fig. 10.14). NBA forms $[Ma - H]^-$ and $Ma^{-\bullet}$ ions. The salt anion contributes the base peak at *m/z* 337.3. $[C + 2A]^-$, *m/z* 697.5, and $[2C + 3A]^-$, *m/z* 1057.6, cluster

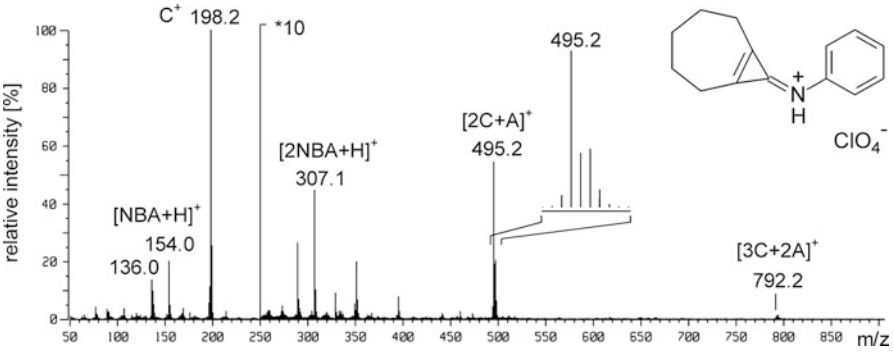

Fig. 10.13 Positive-ion FAB spectrum of an immonium salt [94]. The perchlorate counterion can well be identified from the first and second cluster ion (By courtesy of H. Irngartinger, University of Heidelberg)

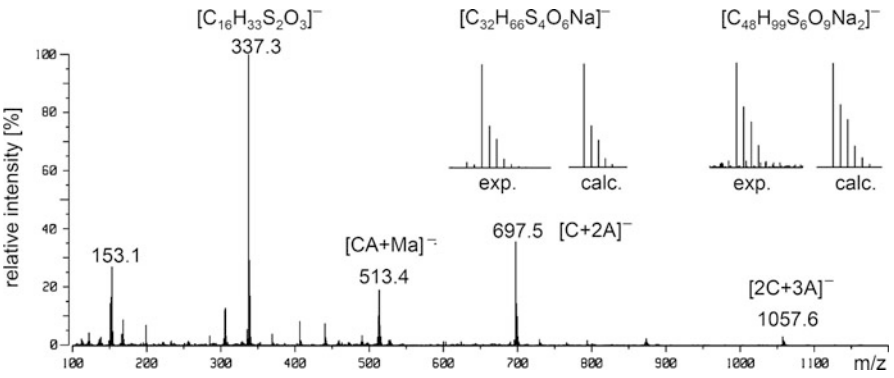

Fig. 10.14 Negative-ion FAB mass spectra of a Bunte salt. The *insets* compare experimental and calculated isotopic patterns of the $[C + 2A]^-$ and $[2C + 3A]^-$ cluster ions (By courtesy of M. Grunze, University of Heidelberg)

ions are observed in addition, their isotopic patterns being in good agreement with theoretical expectation. It is noteworthy that the matrix adduct at *m*/*z* 513.4 is a negative radical ion.

10.6.3 High-Mass Analytes in FAB-MS

FAB is chiefly applied to analytes up to about *m*/*z* 3000, but significantly heavier ions are sometimes accessible. The upper limit surely has been demonstrated by the detection of $[(CsI)_nCs]^+$ cluster ions up to *m*/*z* 90,000 [38]. In case of organic

molecules, $[M + H]^+$, $[M + 2H]^{2+}$, and $[M + 3H]^{3+}$ of porcine trypsin, a protein of $M_r = 23{,}463$ u, have been the highest hitherto detected ions on record [92]. FAB spectra of peptides and small proteins in the m/z 3000–6000 range are more commonly reported [13, 91, 95], and the FAB spectrum of a dendrimer of 7,000 u has also been published [96].

Supramolecular chemistry Inclusion complexes of [60]fullerene, C_{60} [63], of its oxides $C_{60}O$, $C_{60}O_2$, and $C_{60}O_3$ [97], and of several cycloaddition products of the fullerene [98] in γ-cyclodextrin (γ-CD) can be analyzed by negative-ion FAB-MS using "magic bullet" matrix [63]. As one fullerene molecule is enclosed between two γ-CD units, the $[M - H]^-$ ions of these host-guest complexes [99] are detected starting from $[C_{156}H_{159}O_{80}]^-$ (peak of monoisotopic ion expected at m/z 3311.8, Fig. 10.15).

Selecting the matrix
The choice of the matrix is determined by the outer sphere of the analyte molecules, i.e., by γ-CD in case of the above inclusion complexes [60]. Fullerene and its oxides yield poor spectra in "magic bullet", but work well with less polar matrices such as NBA and NPOE.

10.6.4 Accurate Mass Measurements in FAB Mode

FAB produces long-lasting signals of sufficient intensity, thereby allowing to set magnetic sector instruments to 5,000–10,000 resolving power as needed for

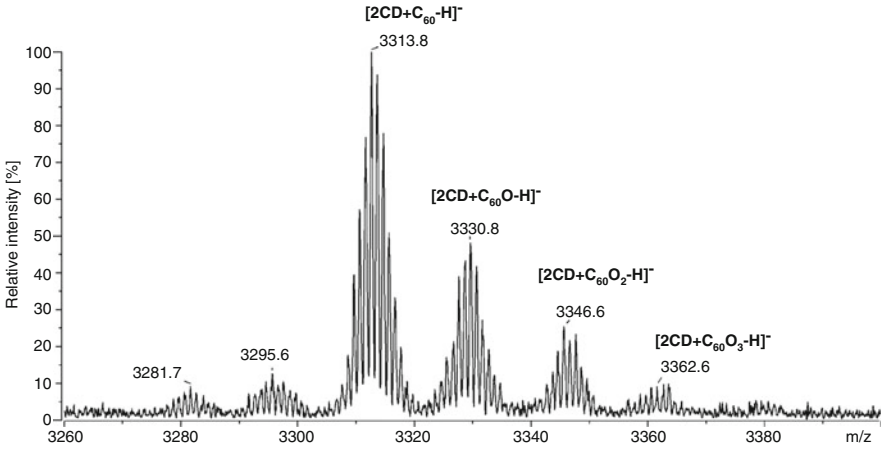

Fig. 10.15 Partial negative-ion FAB spectrum of γ–CD fullerene complexes in "magic bullet" matrix (Reproduced from Ref. [97] by permission. © IM Publications, 1998)

accurate mass measurements. In the range up to about *m*/*z* 600, internal calibration can sometimes be achieved by using the matrix peaks as mass reference, but the admixture of other mass calibrants to the matrix–analyte solution is normally preferred. PEGs are frequently employed for calibration purposes. Then, mass reference peaks are evenly spaced over the *m*/*z* range of interest (44 u distant in case of PEG, cf. Fig. 10.12) and their intensity can be adjusted to approximate those of the analyte. However, the mass calibrant can only be admixed if unwanted reactions with the analyte do not occur. In particular, in case of badly soluble analytes, complete suppression of the analyte signals by the added calibrant may pose a problem.

Accurate mass measurements The positive-ion high-resolution (HR) FAB spectrum of a cationic fluorescent marker dye shows the signal of the analyte ion enclosed by a set of mass reference peaks due to the admixture of PEG 600 (Fig. 10.16). The elemental composition of the analyte can be assigned with good accuracy: exp. *m*/*z* 663.3182, calc. *m*/*z* 663.3153 for $[C_{37}H_{42}O_4N_4F_3]^+$; exp. *m*/*z* 664.3189, calc. *m*/*z* 664.3184 for $[^{13}C^{12}C_{36}H_{42}O_4N_4F_3]^+$.

Provided a (magnetic sector) mass spectrometer offers very good scan-to-scan reproducibility of mass calibration, there is no absolute necessity to admix the mass calibrant to the analyte. Instead, alternating scans on analyte and calibrant offer almost the same level of accuracy. The simplest technical realization of such a *pseudo-internal calibration* is changing the target without interruption of the measurement [100]. The use of a *dual-target* FAB probe (DTP), having a split or double-sided target offering two separated positions, is preferable [101]. Switching between both positions is then achieved by rotating the probe axially between successive scans. The resulting *total ion chromatogram* (TIC) typically has a saw-tooth appearance (Fig. 10.17). Calibration of the analyte spectra is performed by transferring the internal calibration of the mass reference scan(s) to the successive scan(s) on the analyte. The advantages of a DTP are:

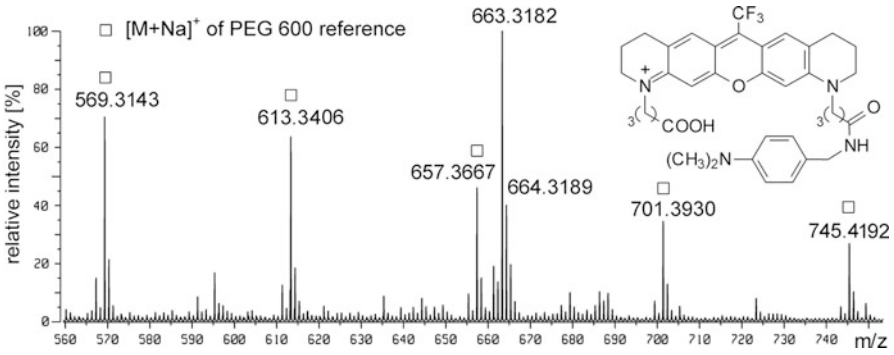

Fig. 10.16 Positive-ion FAB spectrum of a cationic fluorescent marker dye with PEG 600 admixed for internal mass calibration (By courtesy of K. H. Drexhage, University of Siegen and J. Wolfrum, Heidelberg University)

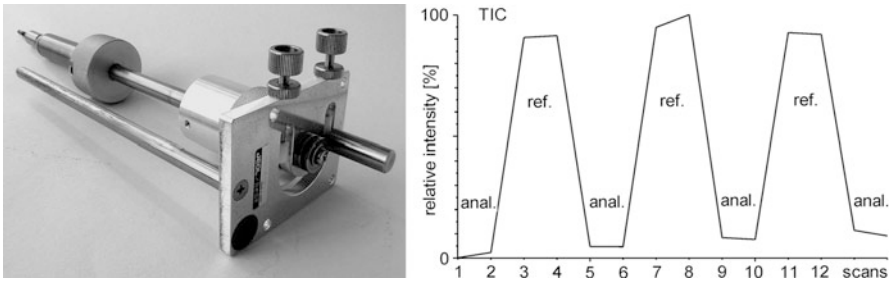

Fig. 10.17 FAB dual-target probe with handle for 180° axial turns (*left*) and TIC of a HR-FAB measurement using this probe (*right*)

- Interference of reference and analyte signals is excluded independent of the resolving power used.
- Mutual suppression of reference and analyte are avoided.
- There is no need to adjust the relative intensities of analyte and calibrant peaks very closely.
- Even otherwise reactive calibrants can be employed due to spatial separation from the analyte [102].

Magnets need time to accommodate
Scanning of a magnet is affected by hysteresis. This improves the reproducibility of mass calibration after several scan cycles. For best results with dual-target probes, it is therefore recommended to skip the first few scans.

10.6.5 Low-Temperature FAB

Originally, cooled FAB probes were designed to prolong the acquisition time for FAB measurements with more volatile matrices [103]. Research on sputtering processes from solid gases [104, 105] and studies of cluster ion formation from solid or deeply cooled liquid alcohols [106–108] have contributed to FAB at cryogenic temperatures [109, 110]. *Low-temperature fast atom bombardment* (LT-FAB) of frozen aqueous solutions of metal salts provides a source of abundant hydrated metal ions [111–113]. Organic molecules can also be detected from their frozen solutions [114]. Such LT-FAB applications are particularly interesting when enabling the detection of species that would otherwise not be accessible by mass spectrometry, because they are either extremely air- and/or water-sensitive [115, 116] as the phosphaoxetane intermediate of the Wittig reaction [117] or insoluble in standard FAB matrices [102, 118].

LT-FAB consumes somewhat higher amounts of sample than FAB at ambient temperature because standard solvents are less effective than conventional

matrices. Thus, the analytes should be dissolved to yield 0.5–3.0 μg μl^{-1} solutions. About 3 μl of solution are deposited on the FAB probe tip and frozen. There are two modes for freezing the sample–matrix mixture: (i) by cooling the target with cold nitrogen gas inside a custom-made vacuum lock before application of the sample [115, 117] or (ii) by simply immersing the target with the drop of solution into liquid nitrogen for about 30 s prior to transfer into the vacuum lock (Fig. 10.18) [102, 109, 110, 116, 119]. LT-FAB mass spectra are then obtained during thawing of frozen solutions inside the FAB ion source, which allows to employ almost any solvent as matrix in LT-FAB-MS. Consequently, neither volatility nor unwanted chemical reactions with the matrix restrict the choice of a matrix. Instead, the solvent matrix may be tailored to the analyte's requirements.

LT-FAB for highly reactive species Selective activation of C–H bonds is rarely observed in saturated alkyl groups. However, iridium complex **1** simply reacts by C–H insertion of the metal into a ligand bond upon treatment with LiBr in solution. The reaction can be tracked by LT-FAB-MS (Fig. 10.19). Decreasing intensity of the molecular ion of **1**, *m*/*z* 812.4, and increasing intensity of $M^{+\bullet}$ of **2**, *m*/*z* 856.4, indicate the progress of this reaction. Furthermore, the halogen exchange is reflected by the changing isotopic pattern.

10.6.6 FAB-MS and Peptide Sequencing

The ability of FAB mass spectra to deliver peptide sequence information was soon recognized [12, 120]. Initially, the sequence was derived from fragment ions observed in the full scan spectra [12, 95]. Another approach to sequence information is to subject the protein to enzymatic hydrolysis by a mixture of several carboxy-peptidases to produce a series of truncated molecules, i.e. of peptides.

Fig. 10.18 Getting ready for LT-FAB by immersion of a FAB target with sample solution into liquid nitrogen. After about 30 s the solvent matrix is deeply frozen and the tip is cooled to allow for transfer of the probe into the vacuum lock and further into the ion source whilst avoiding untimely thawing of the solvent

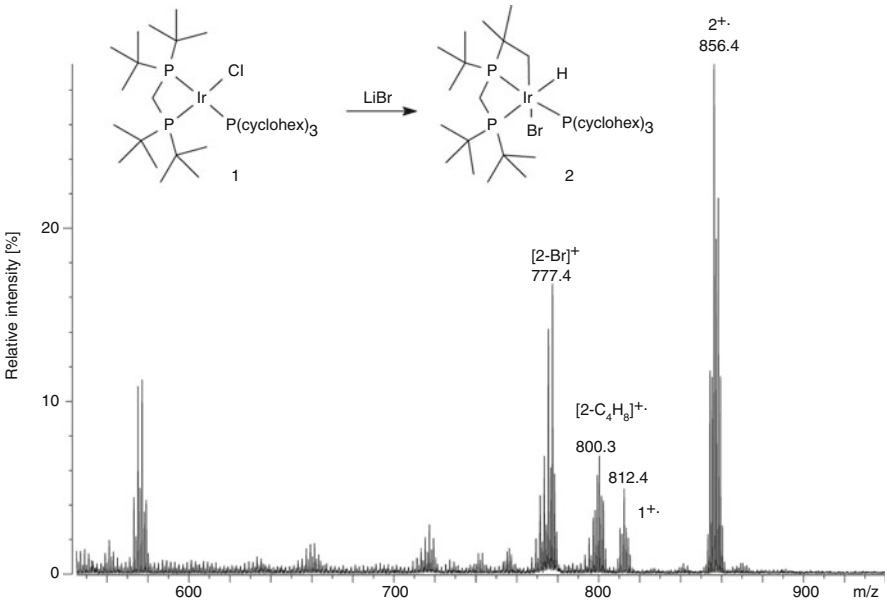

Fig. 10.19 Partial LT-FAB mass spectrum of the reaction mixture containing the iridium complexes **1** and **2** in toluene. In addition to the changes in mass, the isotopic pattern changes upon exchange of Cl by Br (By courtesy of P. Hofmann, Heidelberg University)

The FAB spectrum of the peptide mixture then reveals the *C*-terminal sequence [121, 122]. In the MALDI community, this approach became known as *peptide ladder sequencing* [123].

As protein ions are too big to effect fragmentation by collision-induced dissociation (CID, Sect. 9.3), they are enzymatically degraded to peptides prior to their mass spectrometric examination, e.g., by tryptic digestion [124]. The digest may be used directly to obtain MS/MS spectra of peptide $[M + H]^+$ or $[M + Na]^+$ ions. Alternatively, the peptides may be separated by *liquid chromatography* (LC), *capillary electrophoresis* (CE) [125], or *2D gel electrophoresis* prior to MS.

Nowadays, sequencing of peptides and other biopolymers by tandem mass spectrometry represents a major field of work for many mass spectrometrists [126–129]; FAB and LSIMS no longer play a role here (for an example of peptide sequencing by FAB-MS cf. Sect. 9.6.6).

10.7 FAB and LSIMS: General Characteristics

10.7.1 Sensitivity of FAB-MS

In FAB mode, the sensitivity (Sect. 1.6) is more difficult to specify than for other ionization methods, because the intensity of a signal strongly depends on the actual preparation on the target. Magnetic sector instruments yield ion currents

of about 10^{-11}–10^{-10} A on matrix ions at $R = 1000$. Significantly lower Figs. (10^{-15}–10^{-14} A) are obtained for the $[M + H]^+$ ion of bovine insulin, m/z 5734.6, at $R = 6000$. Accordingly, the detection limits vary depending on the solubility of the analyte and the ease to achieve some sort of ionization if not already ionic at all.

10.7.2 Types of Ions in FAB-MS

FAB produces a variety of ions depending on the polarity and on the ionization energy of the analyte as well as on the presence or absence of impurities such as alkali metal ions [126]. However, with some knowledge of the types of ions formed, reasonable compositions can be assigned to the signals (Table 10.3).

10.7.3 Analytes for FAB-MS

For FAB/LSIMS, the analyte should be soluble to at least 0.1 mg ml^{-1} in some solvent or even better directly in the matrix; concentrations of 0.1–3 μg μl^{-1} in the matrix are ideal. In case of extremely low solubility, additives such as other solvents, acids, or surfactants can help [71].

The analyte may be neutral or ionic. Solutions containing metal salts, e.g., from buffers or excess of non-complexed metals, may cause a confusingly large number of signals due to multiple proton/metal exchange and adduct ion formation [88]. The mass range up to 3,000 u is easily covered by FAB, samples reaching up to about twice that mass still may work if sufficient solubility and some ease of ionization are combined.

Table 10.3 Ions formed by FAB/LSIMS

Analytes	Positive ions	Negative ions
Nonpolar	$M^{+\bullet}$	$M^{-\bullet}$
Medium polarity	$M^{+\bullet}$ and/or $[M + H]^+$, $[M + \text{alkali}]^+$ *Clusters* $[2\ M]^{+\bullet}$ and/or $[2\ M + H]^+$, $[2\ M + \text{alkali}]^+$ *Adducts* $[M + Ma + H]^+$, $[M + Ma + \text{alkali}]^+$	$M^{-\bullet}$ and/or $[M - H]^-$ *Clusters* $[2\ M]^{-\bullet}$ and/or $[2\ M - H]^-$ *Adducts* $[M + Ma]^{-\bullet}$, $[M + Ma - H]^-$
Polar	$[M + H]^+$, $[M + \text{alkali}]^+$ *Clusters* $[nM + H]^+$, $[nM + \text{alkali}]^+$ *Adducts* $[M + Ma + H]^+$, $[M + Ma + \text{alkali}]^+$ *Exchange* $[M - H_n + \text{alkali}_{n+1}]^+$ *High-mass anal.* $[M + 2H]^{2+}$, $[M + 2\text{alkali}]^{2+}$	$[M - H]^-$ *Clusters* $[nM - H]^-$ *Adducts* $[M + Ma - H]^-$ *Exchange* $[M - H_n + \text{alkali}_{n-1}]^-$
Ionic[a]	C^+, $[C_n + A_{n-1}]^+$, rarely $[CA]^{+\bullet}$	A^-, $[C_{n-1} + A_n]^-$, rarely $[CA]^{-\bullet}$

[a]comprising cation C^+ and anion A^-

10.7.4 Mass Analyzers for FAB-MS

Double-focusing magnetic sector instruments represent the standard in FAB-MS, because they combine a suitable mass range with the ability to perform high-resolution and accurate mass measurements. Until the advent of ESI and MALDI, FAB-MS/MS on magnetic four-sector instruments was the method of choice for biomolecule sequencing [130–132]. Linear quadrupole [133] and triple quadrupole instruments have also been adapted to FAB ion sources. Other types of mass analyzers are rare exceptions with FAB or LSIMS ion sources.

10.7.5 Future Perspective for FAB and LSIMS

The strong interrelationship of double-focusing magnetic sector instruments and FAB or LSIMS is most probably the main cause of the extremely diminishing use of this otherwise valuable technique. Clearly, FAB and LSIMs were of highest relevance in the 1990s when the technique had reached maturity (Fig. 10.20). Similarly, as this type of mass analyzer has mostly been replaced by either oaTOF, Orbitrap, or FT-ICR systems, FAB is phasing out from mass spectrometry. This may very well be the last mass spectrometry textbook to include a dedicated chapter on FAB-MS and closely related techniques based on particle impact.

While FAB and LSIMS are highly useful and versatile "soft" methods, they have widely been replaced by matrix-assisted laser desorption/ionization (MALDI,

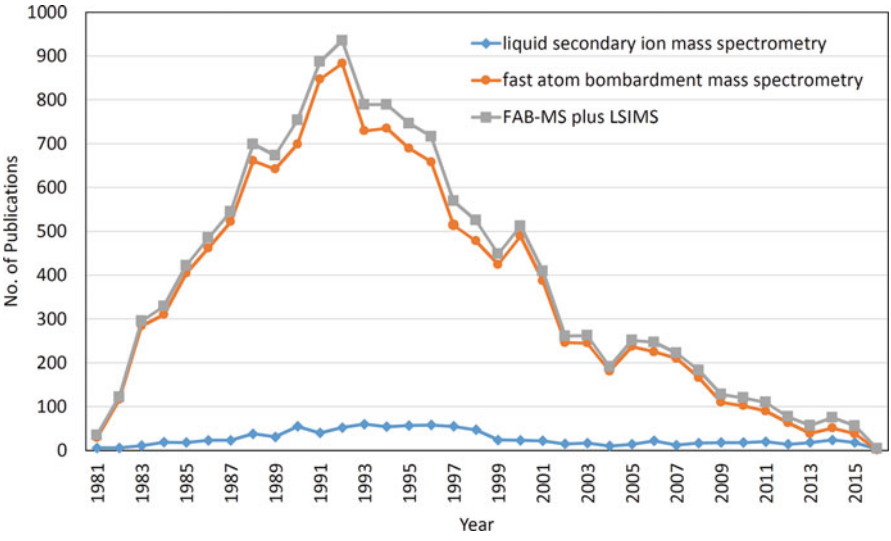

Fig. 10.20 Number of annual publications employing fast atom bombardment mass spectrometry or liquid secondary ion mass spectrometry along with total number of both techniques. Clearly, FAB dominated, while LSIMS had been playing a minor role; both had their greatest impact on MS in the 1990s (Data retrieved using CAS SciFinder software)

Chap. 11), electrospray ionization (ESI, Chap. 12), and related API techniques like atmospheric pressure chemical ionization (APCI), atmospheric pressure photoionization (APPI), direct analysis in real time (DART), and others.

10.8 Massive Cluster Impact

Massive cluster impact (MCI) mass spectrometry presents an additional means of generating secondary ions by bombardment of a surface [25]. Massive clusters of up to 10^8 u are generated by electrohydrodynamic ionization (Sect. 12.1) of an electrolyte/glycerol solution, e.g., 0.75 M ammonium acetate in glycerol. The resulting clusters consisting of about 10^6 glycerol molecules and bearing about 200 electron charges on the average are accelerated by a 10–20 kV high voltage [134]. Although those highly charged microdroplets carry megaelectronvolt kinetic energies, the translational energy per nucleon is only in the order of 1 eV, whereas it is about 50 eV per nucleon in the case of Xe FAB. A shock wave model is proposed to explain ion formation in MCI [135]. According to this model both the impacting cluster and the surface of the bulk or matrix-dissolved analyte are compressed to gigapascal pressures upon impact. Some mixing of analyte and impacting microdroplet can be demonstrated by the occurrence of analyte species cationized by the same ions used as electrolyte in the solution from which the massive clusters are generated. Nonetheless, a matrix effect due to accumulation of a thin layer of glycerol on the surface can be excluded [134]. Instead, dry sample preparations work equally well in MCI [134].

MCI has successfully been applied to analyze proteins up to about 17,000 u [136]. These form multiply charged ions, e.g., $[M + 6Na]^{6+}$, under the conditions of MCI [136]. Especially in the mass range of about 10^4 u, MCI is superior to FAB and LSIMS because it combines good signal intensity due to the enormous momentum of the impinging species with a remarkably low degree of ion fragmentation. Despite of its promising capabilities, MCI has been superseded by MALDI and ESI before it could receive widespread acceptance.

10.9 ^{252}Californium Plasma Desorption

Historically, ^{252}*Californium plasma desorption* (^{252}Cf-PD) was the next desorption /ionization method to be introduced in mass spectrometry after SIMS and MBSA. ^{252}Cf-PD dates back to 1973 [19, 22–24, 137–139] and was the first method to yield ions of bovine insulin [140]. Practically, ^{252}Cf-PD served for protein characterization, an application which is nowadays completely in the hands of MALDI or ESI (Chaps. 11 and 12) [141]. Based on how it was used, PD-MS is rather the precursor of MALDI, based on the principle of ion generation, it is closer to SIMS and FAB.

In ^{252}Cf-PD-MS, particles of megaelectronvolt translational energy are created from radioactive decay of ^{252}Cf nuclides, the nuclear process being the source of their kinetic energy. Each event yields two nuclides of varying identity, the sum of their

masses being the mass of the former nucleus. The fission fragments of similar mass are travelling in opposite directions. Thus, only one of each pair can be employed to effect desorption of ions from a thin film of analyte on a support foil. The ionization process in ^{252}Cf-PD is different from FAB with some closer relations to dry SIMS. The incident particles are normally travelling from the backside through a thin sample layer on a support foil [21, 142]. The initial interaction of the fission fragment with a solid produces approximately 300 electron–hole pairs per angstrom along its track. Recombination of these pairs releases a large amount of energy to the surrounding medium. Within an organic layer, the resulting sudden heat is dissipated by lattice vibrations (phonons) that finally effect desorption of ions from that layer [24, 143, 144]. In addition to spontaneous ion desorption, ionization processes can occur on the nanosecond timescale in the gas phase [145].

Deposition of the analyte on nitrocellulose films instead of metal foils allows the removal of alkali ion contaminations by washing of the sample layer which results in better PD spectra [146]. Further improvements can be achieved by adsorption of the analyte molecules on top of an organic low-molecular-weight matrix layer [147, 148].

Obviously, ^{252}Cf-PD creates ions in a pulsed manner – one burst of ions per fission event – analogous to laser desorption, a fact that restricted the adaptation of ^{252}Cf-PD to time-of-flight (TOF) analyzers (Sect. 4.2). The second fission fragment is not wasted as it serves to trigger the time measurement of the TOF analyzer if the fission fragment source is placed between sample and fission fragment detector (Fig. 10.21) [21, 143].

^{252}Cf-PD mass spectrum of bovine insulin The ^{252}Cf-PD mass spectrum of bovine insulin exhibits the $[M + H]^+$ ion as well as the doubly charged $[M + 2H]^{2+}$ and triply charged $[M + 3H]^{3+}$ ion (Fig. 10.22) [139]. In addition, there are fragment ions corresponding to the A and B chain as well as some **a**-type peptide fragments ions.

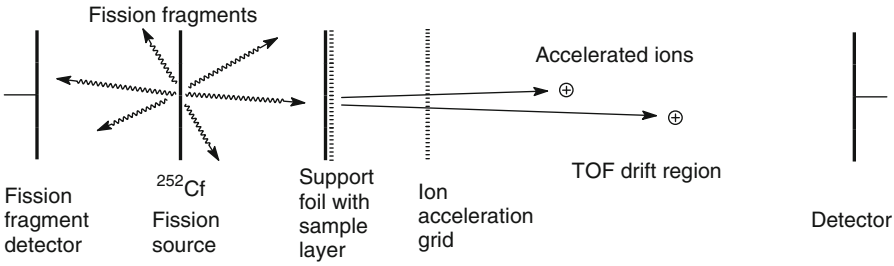

Fig. 10.21 Schematic of a ^{252}Cf-plasma desorption TOF instrument [143]

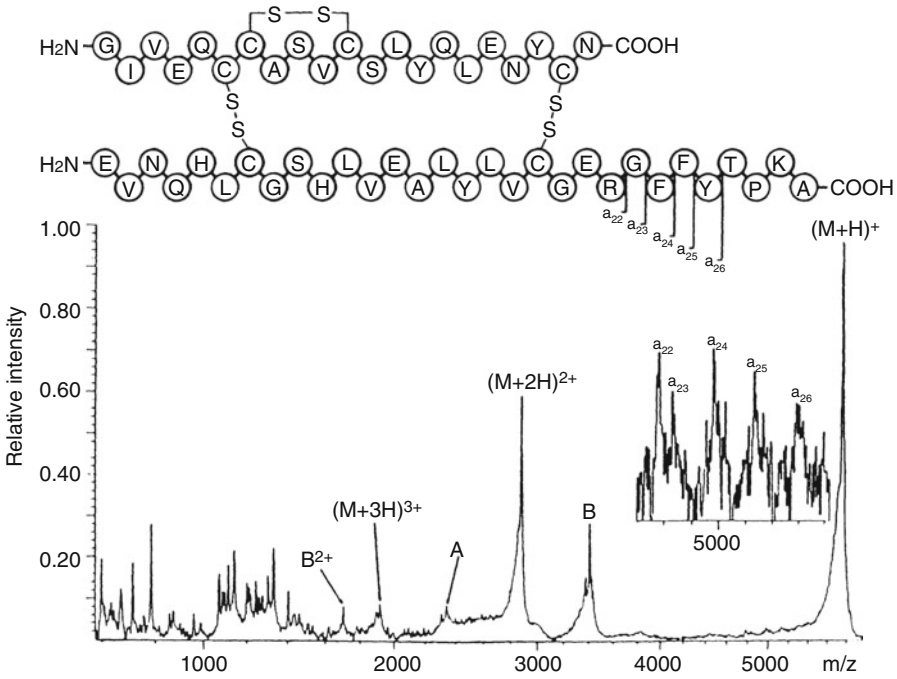

Fig. 10.22 ^{252}Cf-PD mass spectrum of oxidized insulin. Note the extremely uneven baseline and the tailing of the peaks towards the low-mass side, which is due to fragmentation (Reproduced from Ref. [139] by permission. © John Wiley and Sons, 1994)

10.10 Ionization by Particle Impact at a Glance

Basic Principle

The ionization techniques discussed in this chapter share the feature that they all rely on the impact of energetic primary particles to effect ablation and eventually ionization of neutrals. These techniques include *secondary ion mass spectrometry* (SIMS), *^{252}Californium* (^{252}Cf) *plasma desorption* (PD), *molecular beam solid analysis* (MBSA), *fast atom bombardment* (FAB), and *liquid secondary ion mass spectrometry* (LSIMS). SIMS paved the way to all the other mentioned techniques. SIMS uses primary ions to induce the generation of secondary ions and still is profitably used in inorganic MS, most importantly, for imaging applications (Sect. 15.6). MBSA was the first method to use a primary beam of neutrals and was later established in organic MS as FAB. The versatility and softness of FAB is based on the use of a liquid matrix, which acts as a solvent for the analyte and as a moderator for the energy of the primary neutrals. Other than employing primary ions, SIMS is practically identical to FAB.

Analytes for FAB and LSIMS

Analytes need to be soluble in the organic solvent matrix. FAB and LSIMS likewise can be employed for nonpolar, polar, and ionic analytes. Exposure of a

drop of the analyte–matrix mixture to the primary beam is performed on the tip of a probe.

Analytes should preferably be soluble in standard solvents including DMF and DMSO. Solutions of 0.3–3.0 mg ml^{-1} are suitable for admixture to the matrix. FAB and LSIMS are capable of analyzing molecules up to 2,000–4,000 u, depending on their solubility in the matrix. Low-mass analytes may interfere with matrix peaks.

Analytes for PD-MS
PD-MS has been used to analyze (bio)macromolecules. PD-MS is strictly linked to TOF analyzers and requires dedicated instruments. With the advent of ESI and MALDI, PD-MS has essentially disappeared from practical use.

Polarity
FAB and LSIMS both generate positive as well as negative ions. The analyte can be detected as molecular ions or adduct ions, e.g., $M^{+\bullet}$, $[M + H]^+$, $[M + cation]^+$, $M^{-\bullet}$, $[M - H]^-$, $[M + anion]^-$. The choice of ion polarity is usually based on the properties of the analyte, i.e., depends on its acidity or basicity, ionization energy or electron affinity.

Softness of Ionization
FAB and LSIMS are soft desorption/ionization methods. Often, only species reflecting the intact analyte molecule are observed. The softness of ionization allows for matrix adduct ions to occur. Nonetheless, some fragmentation can occasionally be observed as a result of energy imparted onto the ions by collisions in the selvedge region between condensed phase and gas phase.

Instrumentation
Magnetic sector instruments are normally used in combination with FAB and LSIMS. The fact that this type of mass analyzer is vanishing from organic and life science MS laboratories causes FAB and LSIMS to disappear from the repertoire of ionization methods in use.

Accurate Mass
Due to stable and long-lasting ion currents, FAB and LISMS are well suited for high-resolution and accurate mass measurements. Internal mass calibration is required when magnetic sector instruments are used. Often, it is just sufficient to admix a calibration compound to the analyte–matrix solution. If admixture cannot be achieved, dual target probes provide pseudo-internal calibration.

Dissemination and Availability
In the late 1980s and 1990s, magnetic sector instruments were sold with FAB or LSIMS as optional ionization methods. Nowadays, FAB and LSIMS have mostly been superseded by ESI, APCI, MALDI, and also by ambient ionization techniques.

References

1. Benninghoven A (2011) The Development of SIMS and International SIMS Conferences: A Personal Retrospective View. Surf Interface Anal 43:2–11. doi:10.1002/sia.3688

2. Honig RE (1985) The Development of Secondary Ion Mass Spectrometry (SIMS): a Retrospective. Int J Mass Spectrom Ion Proc 66:31–54. doi:10.1016/0168-1176(85)83018-4
3. Honig RE (1995) Stone-Age Mass Spectrometry: The Beginnings of "SIMS" at RCA Laboratories, Princeton. Int J Mass Spectrom Ion Proc 143:1–10. doi:10.1016/0168-1176(94)04130-Y
4. Barber M, Vickerman JC, Wolstenholme J (1980) Secondary Ion Mass Spectra of Some Simple Organic Molecules. J Chem Soc Faraday Trans 1(76):549–559. doi:10.1039/F19807600549
5. Benninghoven A (1983) Secondary ion mass spectrometry of organic compounds. In: Benninghoven A (ed) Ion Formation from Organic Solids. Springer, Heidelberg
6. Devienne FM (1967) Different Uses of High Energy Molecular Beams. Entropie 18:61–67
7. Devienne FM, Roustan JC (1982) "Fast Atom Bombardment" – A Rediscovered Method for Mass Spectrometry. Org Mass Spectrom 17:173–181. doi:10.1002/oms.1210170405
8. Barber M, Bordoli RS, Sedgwick RD, Tyler AN (1981) Fast Atom Bombardment of Solids as an Ion Source in Mass Spectrometry. Nature 293:270–275. doi:10.1038/293270a0
9. Barber M, Bordoli RS, Sedgwick RD, Tyler AN (1981) Fast Atom Bombardment Mass Spectrometry of Cobalamines. Biomed Mass Spectrom 8:492–495. doi:10.1002/bms.1200081005
10. Surman DJ, Vickerman JC (1981) Fast Atom Bombardment Quadrupole Mass Spectrometry. J Chem Soc Chem Commun:324–325. doi:10.1039/C39810000324
11. Barber M, Bordoli RS, Sedgwick RD, Tyler AN, Bycroft BW (1981) Fast Atom Bombardment Mass Spectrometry of Bleomycin A2 and B2 and Their Metal Complexes. Biochem Biophys Res Commun 101:632–638. doi:10.1016/0006-291X(81)91305-X
12. Morris HR, Panico M, Barber M, Bordoli RS, Sedgwick RD, Tyler AN (1981) Fast Atom Bombardment: A New Mass Spectrometric Method for Peptide Sequence Analysis. Biochem Biophys Res Commun 101:623–631. doi:10.1016/0006-291X(81)91304-8
13. Barber M, Bordoli RS, Elliott GJ, Sedgwick RD, Tyler AN, Green BN (1982) Fast Atom Bombardment Mass Spectrometry of Bovine Insulin and Other Large Peptides. J Chem Soc Chem Commun:936–938. doi:10.1039/C39820000936
14. Barber M, Bordoli RS, Elliott GJ, Sedgwick RD, Tyler AN (1982) Fast Atom Bombardment Mass Spectrometry. Anal Chem 54:645A–657A. doi:10.1021/ac00241a817
15. Meili J, Seibl J (1983) Matrix Effects in Fast Atom Bombardment (FAB) Mass Spectrometry. Int J Mass Spectrom Ion Phys 46:367–370. doi:10.1016/0020-7381(83)80128-4
16. Gower LJ (1985) Matrix Compounds for Fast Atom Bombardment Mass Spectrometry. Biomed Mass Spectrom 12:191–196. doi:10.1002/bms.1200120502
17. De Pauw E, Agnello A, Derwa F (1991) Liquid Matrices for Liquid Secondary Ion Mass Spectrometry-Fast Atom Bombardment [LSIMS-FAB]: An Update. Mass Spectrom Rev 10:283–301. doi:10.1002/mas.1280100402
18. Aberth W, Straub KM, Burlingame AL (1982) Secondary Ion Mass Spectrometry with Cesium Ion Primary Beam and Liquid Target Matrix for Analysis of Bioorganic Compounds. Anal Chem 54:2029–2034. doi:10.1021/ac00249a028
19. Sundqvist BUR (1992) Desorption Methods in Mass Spectrometry. Int J Mass Spectrom Ion Proc 118(119):265–287. doi:10.1016/0168-1176(92)85065-8
20. Sunner J (1993) Ionization in Liquid Secondary Ion Mass Spectrometry (LSIMS). Org Mass Spectrom 28:805–823. doi:10.1002/oms.1210280802
21. Busch KL (1995) Desorption Ionization Mass Spectrometry. J Mass Spectrom 30:233–240. doi:10.1002/jms.1190300202
22. Macfarlane RD, Torgerson DF (1976) Californium-252-Plasma Desorption Time-of-Flight Mass Spectrometry. Int J Mass Spectrom Ion Phys 21:81–92. doi:10.1016/0020-7381(76)80068-X
23. Macfarlane RD, Torgerson DF (1976) Californium-252 Plasma Desorption Mass Spectroscopy. Science 191:920–925. doi:10.1126/science.1251202

24. Macfarlane RD (1983) High energy heavy-ion induced desorption. In: Benninghoven A (ed) Ion Formation from Organic Solids. Springer, Heidelberg
25. Mahoney JF, Perel J, Ruatta SA, Martino PA, Husain S, Lee TD (1991) Massive Cluster Impact Mass Spectrometry: A New Desorption Method for the Analysis of Large Biomolecules. Rapid Commun Mass Spectrom 5:441–445. doi:10.1002/rcm.1290051004
26. Miller JM (1989) Fast Atom Bombardment Mass Spectrometry of Organometallic, Coordination, and Related Compounds. Mass Spectrom Rev 9:319–347. doi:10.1002/mas.1280090304
27. Franks J, Ghander AM (1974) Saddle Field Ion Source of Spherical Configuration for Etching and Thinning Applications. Vacuum 24:489–491. doi:10.1016/0042-207X(74)90015-3
28. Alexander AJ, Hogg AM (1986) Characterization of a Saddle-Field Discharge Gun for FABMS Using Different Discharge Vapors. Int J Mass Spectrom Ion Proc 69:297–311. doi:10.1016/0168-1176(86)87021-5
29. Boggess B, Cook KD (1994) Determination of Flux from a Saddle Field Fast-Atom Bombardment Gun. J Am Soc Mass Spectrom 5:100–105. doi:10.1016/1044-0305(94)85041-0
30. Barber M, Bordoli RS, Sedgwick RD, Tyler AN (1981) Fast Atom Bombardment of Solids (F.A.B.): A New Ion Source for Mass Spectrometry. J Chem Soc Chem Commun 7:325–327. doi:10.1039/C39810000325
31. McDowell RA, Morris HR (1983) Fast Atom Bombardment Mass Spectrometry: Biological Analysis Using an Ion Gun. Int J Mass Spectrom Ion Phys 46:443–446. doi:10.1016/0020-7381(83)80147-8
32. Morris HR, Panico M, Haskins NJ (1983) Comparison of Ionization Gases in FAB Mass Spectra. Int J Mass Spectrom Ion Phys 46:363–366. doi:10.1016/0020-7381(83)80127-2
33. Fenselau C (1983) Fast Atom Bombardment. In: Benninghoven A (ed) Ion Formation from Organic Solids. Springer, Heidelberg
34. Burlingame AL, Aberth W (1983) Use of a cesium primary beam for liquid SIMS analysis of bio-organic compounds. In: Benninghoven A (ed) Ion Formation from Organic Solids. Springer, Heidelberg
35. Aberth W, Burlingame AL (1984) Comparison of Three Geometries for a Cesium Primary Beam Liquid Secondary Ion Mass Spectrometry Source. Anal Chem 56:2915–2918. doi:10.1021/ac00278a066
36. Aberth WH, Burlingame AL (1988) Effect of Primary Beam Energy on the Secondary-Ion Sputtering Efficiency of Liquid Secondary-Ionization Mass Spectrometry in the 5–30-keV Range. Anal Chem 60:1426–1428. doi:10.1021/ac00165a016
37. McEwen CN, Hass JR (1985) Negative Gold Ion Gun for Liquid Secondary Ion Mass Spectrometry. Anal Chem 57:890–892. doi:10.1021/ac00281a025
38. Katakuse I, Nakabushi H, Ichihara T, Sakurai T, Matsuo T, Matsuda H (1984) Generation and Detection of Cluster Ions $[(CsI)_NCs]^+$ Ranging up to $m/z = 90{,}000$. Int J Mass Spectrom Ion Proc 57:239–243. doi:10.1016/0168-1176(84)85180-0
39. Katakuse I, Nakabushi H, Ichihara T, Sakurai T, Matsuo T, Matsuda H (1984) Metastable Decay of Cesium Iodide Cluster Ions. Int J Mass Spectrom Ion Proc 62:17–23. doi:10.1016/0168-1176(84)80066-X
40. Sim PG, Boyd RK (1991) Calibration and Mass Measurement in Negative-Ion Fast-Atom Bombardment Mass Spectrometry. Rapid Commun Mass Spectrom 5:538–542. doi:10.1002/rcm.1290051111
41. Rapp U, Kaufmann H, Höhn M, Pesch R (1983) Exact Mass Determinations Under FAB Conditions. Int J Mass Spectrom Ion Phys 46:371–374. doi:10.1016/0020-7381(83)80129-6
42. Sunner J (1993) Role of Ion-Ion Recombination for Alkali Chloride Cluster Formation in Liquid Secondary Ion Mass Spectrometry. J Am Soc Mass Spectrom 4:410–418. doi:10.1016/1044-0305(93)85006-J
43. Cao Y, Haseltine JN, Busch KL (1996) Double Cationization with Alkali Ions in Liquid Secondary Ion Mass Spectrometry. Spectroscopy Lett 29:583–589. doi:10.1080/00387019608007053

44. Todd PJ (1988) Secondary Ion Emission from Glycerol Under Continuous and Pulsed Primary Ion Current. Org Mass Spectrom 23:419–424. doi:10.1002/oms.1210230521
45. Schröder E, Münster H, Budzikiewicz H (1986) Ionization by Fast Atom Bombardment - a Chemical Ionization (Matrix) Process Ion the Gas Phase? Org Mass Spectrom 21:707–715. doi:10.1002/oms.1210211016
46. Münster H, Theobald F, Budzikiewicz H (1987) The Formation of a Matrix Plasma in the Gas Phase Under Fast Atom Bombardment Conditions. Int J Mass Spectrom Ion Proc 79:73–79. doi:10.1016/0168-1176(87)80024-1
47. Rosen RT, Hartmann TG, Rosen JD, Ho CT (1988) Fast-Atom-Bombardment Mass Spectra of Low-Molecular-Weight Alcohols and Other Compounds. Evidence for a Chemical-Ionization Process in the Gas Phase. Rapid Commun Mass Spectrom 2:21–23. doi:10.1002/rcm.1290020108
48. Miller JM, Balasanmugam K (1989) Fast Atom Bombardment Mass Spectrometry of Some Nonpolar Compounds. Anal Chem 61:1293–1295. doi:10.1021/ac00186a022
49. Benninghoven A (1983) Organic Secondary Ion Mass Spectrometry (SIMS) and Its Relation to Fast Atom Bombardment (FAB). Int J Mass Spectrom Ion Phys 46:459–462. doi:10.1016/0020-7381(83)80151-X
50. van Breemen RB, Snow M, Cotter RJ (1983) Time-Resolved Laser Desorption Mass Spectrometry. I. Desorption of Preformed Ions. Int J Mass Spectrom Ion Phys 49:35–50. doi:10.1016/0020-7381(83)85074-8
51. Musselman B, Watson JT, Chang CK (1986) Direct Evidence for Preformed Ions of Porphyrins in the Solvent Matrix for Fast Atom Bombardment Mass Spectrometry. Org Mass Spectrom 21:215–219. doi:10.1002/oms.1210210408
52. Shiea J, Sunner J (1991) The Acid Effect in Fast Atom Bombardment. Org Mass Spectrom 26:38–44. doi:10.1002/oms.1210260107
53. Todd PJ (1991) Solution Chemistry and Secondary Ion Emission from Amine-Glycerol Solutions. J Am Soc Mass Spectrom 2:33–44. doi:10.1016/1044-0305(91)80059-G
54. Wong SS, Röllgen FW (1986) Sputtering of Large Molecular Ions by Low Energy Particle Impact. Nulc Instrum Methods Phys Res B B14:436–447. doi:10.1016/0168-583X(86)90139-4
55. Baczynskyi L (1985) New Matrices for Fast Atom Bombardment Mass Spectrometry. Adv Mass Spectrom 10:1611–1612
56. De Pauw E, Agnello A, Derwa F (1986) Liquid Matrices for Liquid Secondary Ion Mass Spectrometry. Mass Spectrom Rev 5:191–212. doi:10.1002/mas.1280050204
57. Gower LJ (1985) Matrix Compounds for Fast Atom Bombardment: A Further Review. Adv Mass Spectrom 10:1537–1538
58. Staempfli AA, Schlunegger UP (1991) A New Matrix for Fast-Atom Bombardment Analysis of Corrins. Rapid Commun Mass Spectrom 5:30–31. doi:10.1002/rcm.1290050108
59. Visentini J, Nguyen PM, Bertrand MJ (1991) The Use of 4-Hydroxybenzenesulfonic Acid as a Reduction-Inhibiting Matrix in Liquid Secondary-Ion Mass Spectrometry. Rapid Commun Mass Spectrom 5:586–590. doi:10.1002/rcm.1290051204
60. Meili J, Seibl J (1984) A New Versatile Matrix for Fast Atom Bombardment Analysis. Org Mass Spectrom 19:581–582. doi:10.1002/oms.1210191111
61. Barber M, Bell D, Eckersley M, Morris M, Tetler L (1988) The Use of *meta*-Nitrobenzyl Alcohol as a Matrix in Fast Atom Bombardment Mass Spectrometry. Rapid Commun Mass Spectrom 2:18–21. doi:10.1002/rcm.1290020107
62. Aubagnac J-L (1990) Use of *M*-Nitrobenzyl Alcohol As a Matrix in Fast-Atom-Bombardment Negative-Ion Mass Spectrometry of Polar Compounds. Rapid Commun Mass Spectrom 4:114–116. doi:10.1002/rcm.1290040405
63. Andersson T, Westman G, Stenhagen G, Sundahl M, Wennerström O (1995) A Gas Phase Container for C_{60}: a γ-Cyclodextrin Dimer. Tetrahedron Lett 36:597–600. doi:10.1016/0040-4039(94)02282-G

64. Dube G (1984) The Behavior of Aromatic Hydrocarbons Under Fast Atom Bombardment. Org Mass Spectrom 19:242–243. doi:10.1002/oms.1210190510
65. Abdul-Sada AK, Greenway AM, Seddon KR (1989) The Extent of Aggregation of Air-Sensitive Alkyllithium Compounds as Determined by Fast-Atom-Bombardment Mass Spectrometry. J Organomet Chem 375:C17–C19. doi:10.1016/0022-328X(89)85099-5
66. Abdul-Sada AK, Greenway AM, Seddon KR (1996) The Application of Liquid Paraffin and 3,4-Dimethoxybenzyl Alcohol as Matrix Compounds to Fast Atom Bombardment Mass Spectrometry. Eur Mass Spectrom 2:77–78. doi:10.1255/ejms.82
67. Bandini AL, Banditelli G, Minghetti G, Pelli B, Traldi P (1989) Fast Atom Bombardment Induced Decomposition Pattern of the Gold(III) Bis(Carbene) Complex $[[(p\text{-}MeC_6H_4NH)(EtO)C]_2AuI_2]ClO_4$, a Retrosynthetic Process? Organometallics 8:590–593. doi:10.1021/om00105a003
68. Dobson JC, Taube H (1989) Coordination Chemistry and Redox Properties of Polypyridyl Complexes of Vanadium(II). Inorg Chem 28:1310–1315. doi:10.1021/ic00306a021
69. Leibman CP, Todd PJ, Mamantov G (1988) Enhanced Positive Secondary Ion Emission from Substituted Polynuclear Aromatic Hydrocarbon/Sulfuric Acid Solutions. Org Mass Spectrom 23:634–642. doi:10.1002/oms.1210230903
70. Rozenski J, Herdewijn P (1995) The Effect of Addition of Carbon Powder to Samples in Liquid Secondary Ion Mass Spectrometry: Improved Ionization of Apolar Compounds. Rapid Commun Mass Spectrom 9:1499–1501. doi:10.1002/rcm.1290091507
71. Huang ZH, Shyong BJ, Gage DA, Noon KR, Allison J (1994) *N*-Alkylnicotinium Halides: A Class of Cationic Matrix Additives for Enhancing the Sensitivity in Negative Ion Fast-Atom Bombardment Mass Spectrometry of Polyanionic Analytes. J Am Soc Mass Spectrom 5:935–948. doi:10.1016/1044-0305(94)87019-5
72. Shiea JT, Sunner J (1990) Effects of Matrix Viscosity on FAB Spectra. Int J Mass Spectrom Ion Proc 96:243–265. doi:10.1016/0168-1176(90)85126-M
73. Field FH (1982) Fast Atom Bombardment Study of Glycerol: Mass Spectra and Radiation Chemistry. J Phys Chem 86:5115–5123. doi:10.1021/j100223a013
74. Caldwell KA, Gross ML (1994) Origins and Structures of Background Ions Produced by Fast-Atom Bombardment of Glycerol. J Am Soc Mass Spectrom 5:72–91. doi:10.1016/1044-0305(94)85039-9
75. Busch KL (2002) Chemical Noise in Mass Spectrometry. Part I. Spectroscopy 17:32–37
76. Busch KL (2003) Chemical Noise in Mass Spectrometry. Part II – Effects of Choices in Ionization Methods on Chemical Noise. Spectroscopy 18:56–62
77. Reynolds JD, Cook KD (1990) Improving Fast Atom Bombardment Mass Spectra: the Influence of Some Controllable Parameters on Spectral Quality. J Am Soc Mass Spectrom 1:149–157. doi:10.1016/1044-0305(90)85051-M
78. Barber M, Bell DJ, Morris M, Tetler LW, Woods MD, Monaghan JJ, Morden WE (1988) The Interaction of *meta*-Nitrobenzyl Alcohol with Compounds Under Fast-Atom-Bombardment Conditions. Rapid Commun Mass Spectrom 2:181–183. doi:10.1002/rcm.1290020905
79. Tuinman AA, Cook KD (1992) Fast Atom Bombardment-Induced Condensation of Glycerol with Ammonium Surfactants. I. Regioselectivity of the Adduct Formation. J Am Soc Mass Spectrom 3:318–325. doi:10.1016/1044-0305(92)87059-8
80. Aubagnac JL, Claramunt RM, Sanz D (1990) Reduction Phenomenon on the FAB Mass Spectra of *N*-Aminoazoles with a Glycerol Matrix. Org Mass Spectrom 25:293–295. doi:10.1002/oms.1210250511
81. Murthy VS, Miller JM (1993) Suppression Effects on a Reduction Process in Fast-Atom Bombardment Mass Spectrometry. Rapid Commun Mass Spectrom 7:874–881. doi:10.1002/rcm.1290071004
82. Aubagnac J-L, Gilles I, Lazaro R, Claramunt R-M, Gosselin G, Martinez J (1995) Reduction Phenomenon in Frit Fast-Atom Bombardment Mass Spectrometry. Rapid Commun Mass Spectrom 9:509–511. doi:10.1002/rcm.1290090607

83. Aubagnac J-L, Gilles I, Claramunt RM, Escolastico C, Sanz D, Elguero J (1995) Reduction of Aromatic Fluorine Compounds in Fast-Atom Bombardment Mass Spectrometry. Rapid Commun Mass Spectrom 9:156–159. doi:10.1002/rcm.1290090210
84. Théberge R, Bertrand MJ (1995) Beam-Induced Dehalogenation in LSIMS: Effect of Halogen Type and Matrix Chemistry. J Mass Spectrom 30:163–171. doi:10.1002/jms.1190300125
85. Théberge R, Bertrand MJ (1998) An Investigation of the Relationship Between Analyte Surface Concentration and the Extent of Beam-Induced Dehalogenation in Liquid Secondary Ion Mass Spectrometry. Rapid Commun Mass Spectrom 12:2004–2010. doi:10.1002/(SICI)1097-0231(19981230)12:24<2004::AID-RCM427>3.0.CO;2-P
86. Vetter W, Meister W (1985) Fast Atom Bombardment Mass Spectrum of β-Carotene. Org Mass Spectrom 20:266–267. doi:10.1002/oms.1210200321
87. Nakata H, Tanaka K (1994) Structural and Substituent Effects on $M^{+\cdot}$ vs. $[M + H]^+$ Formation in Fast Atom Bombardment Mass Spectra of Simple Organic Compounds. Org Mass Spectrom 29:283–288. doi:10.1002/oms.1210290604
88. Moon DC, Kelly JA (1988) A Simple Desalting Procedure for Fast Atom Bombardment Mass Spectrometry. Biomed Mass Spectrom 17:229–237. doi:10.1002/bms.1200170312
89. Prókai L, Hsu BH, Farag H, Bodor N (1989) Desorption Chemical Ionization, Thermospray, and Fast Atom Bombardment Mass Spectrometry of Dihydropyridine – Pyridinium Salt-Type Redox Systems. Anal Chem 61:1723–1728. doi:10.1021/ac00190a026
90. Kolli VSK, York WS, Orlando R (1998) Fast Atom Bombardment Mass Spectrometry of Carbohydrates Contaminated with Inorganic Salts Using a Crown Ether. J Mass Spectrom 33:680–682. doi:10.1002/(SICI)1096-9888(199807)33:7<680::AID-JMS673>3.0.CO;2-Y
91. Desiderio DM, Katakuse I (1984) Fast Atom Bombardment Mass Spectrometry of Insulin, Insulin A-Chain, Insulin B-Chain, and Glucagon. Biomed Mass Spectrom 11:55–59. doi:10.1002/bms.1200110202
92. Barber M, Green BN (1987) The Analysis of Small Proteins in the Molecular Weight Range 10–24 kDa by Magnetic Sector Mass Spectrometry. Rapid Commun Mass Spectrom 1:80–83. doi:10.1002/rcm.1290010505
93. Frauenkron M, Berkessel A, Gross JH (1997) Analysis of Ruthenium Carbonyl-Porphyrin Complexes: A Comparison of Matrix-Assisted Laser Desorption/Ionization Time-of-Flight, Fast-Atom Bombardment and Field Desorption Mass Spectrometry. Eur Mass Spectrom 3:427–438. doi:10.1255/ejms.177
94. Irngartinger H, Altreuther A, Sommerfeld T, Stojanik T (2000) Pyramidalization in Derivatives of Bicyclo[5.1.0]oct-1(7)-enes and 2,2,5,5-Tetramethylbicyclo[4.1.0]hept-1(6)-enes. Eur J Org Chem 2000:4059–4070. doi:10.1002/1099-0690(200012)2000:24<4059::AID-EJOC4059>3.0.CO;2-V
95. Barber M, Bordoli RS, Elliott GJ, Tyler AN, Bill JC, Green BN (1984) Fast Atom Bombardment (FAB) Mass Spectrometry: A Mass Spectral Investigation of Some of the Insulins. Biomed Mass Spectrom 11:182–186. doi:10.1002/bms.1200110409
96. Rajca A, Wongsriratanakul J, Rajca S, Cerny R (1998) A Dendritic Macrocyclic Organic Polyradical with a Very High Spin of $S = 10$. Angew Chem Int Ed 37:1229–1232. doi:10.1002/(SICI)1521-3773(19980518)37:9<1229::AID-ANIE1229>3.0.CO;2-%23
97. Giesa S, Gross JH, Krätschmer W, Gleiter R (1998) Experiments Towards an Analytical Application of Host-Guest Complexes of [60] Fullerene and Its Derivatives. Eur Mass Spectrom 4:189–196. doi:10.1255/ejms.208
98. Juo CG, Shiu LL, Shen CKF, Luh TJ, Her GR (1995) Analysis of C_{60} Derivatives by Fast-Atom Bombardment Mass Spectrometry As Γ-Cyclodextrin Inclusion Complexes. Rapid Commun Mass Spectrom 9:604–608. doi:10.1002/rcm.1290090714
99. Vincenti M (1995) Host-Guest Chemistry in the Mass Spectrometer. J Mass Spectrom 30:925–939. doi:10.1002/jms.1190300702
100. Morgan RP, Reed ML (1982) Fast Atom Bombardment (FAB)-Accurate Mass Measurement. Org Mass Spectrom 17:537. doi:10.1002/oms.1210171015

101. Münster H, Budzikiewicz H, Schröder E (1987) A Modified Target for FAB Measurements. Org Mass Spectrom 22:384–385. doi:10.1002/oms.1210220616
102. Gross JH, Giesa S, Krätschmer W (1999) Negative-Ion Low-Temperature Fast-Atom Bombardment Mass Spectrometry of Monomeric and Dimeric [60]Fullerene Compounds. Rapid Commun Mass Spectrom 13:815–820. doi:10.1002/(SICI)1097-0231(19990515)13:9<815::AID-RCM572>3.0.CO;2-L
103. Falick AM, Walls FC, Laine RA (1986) Cooled Sample Introduction Probe for Liquid Secondary Ionization Mass Spectrometry. Anal Biochem 159:132–137. doi:10.1016/0003-2697(86)90317-9
104. Jonkman HT, Michl J (1981) Secondary Ion Mass Spectrometry of Small-Molecule Solids at Cryogenic Temperatures. 1. Nitrogen and Carbon Monoxide. J Am Chem Soc 103:733–737. doi:10.1021/ja00394a001
105. Orth RG, Jonkman HT, Michl J (1981) Secondary Ion Mass Spectrometry of Small-Molecule Solids at Cryogenic Temperatures. 2. Rare Gas Solids. J Am Chem Soc 103:6026–6030. doi:10.1021/ja00410a006
106. Katz RN, Chaudhary T, Field FH (1986) Particle Bombardment (FAB) Mass Spectra of Methanol at Sub-Ambient Temperatures. J Am Chem Soc 108:3897–3903. doi:10.1021/ja00274a007
107. Katz RN, Chaudhary T, Field FH (1987) Particle Bombardment (KeV) Mass Spectra of Ethylene Glycol, Glycerol, and Water at Sub-Ambient Temperatures. Int J Mass Spectrom Ion Proc 78:85–97. doi:10.1016/0168-1176(87)87043-X
108. Johnstone RAW, Wilby AH (1989) Fast Atom Bombardment at Low Temperatures. Part 2. Polymerization in the Matrix. Int J Mass Spectrom Ion Proc 89:249–264. doi:10.1016/0168-1176(89)83063-0
109. Kosevich MV, Czira G, Boryak OA, Shelkovsky VS, Vékey K (1997) Comparison of Positive and Negative Ion Clusters of Methanol and Ethanol Observed by Low Temperature Secondary Ion Mass Spectrometry. Rapid Commun Mass Spectrom 11:1411–1416. doi:10.1002/(SICI)1097-0231(19970830)11:13<1411::AID-RCM967>3.0.CO;2-8
110. Kosevich MV, Czira G, Boryak OA, Shelkovsky VS, Vékey K (1998) Temperature Dependences of Ion Currents of Alcohol Clusters Under Low-Temperature Secondary Ion Mass Spectrometric Conditions. J Mass Spectrom 33:843–849. doi:10.1002/(SICI)1096-9888(199809)33:9<843::AID-JMS695>3.0.CO;2-7
111. Magnera TF, David DE, Stulik D, Orth RG, Jonkman HT, Michl J (1989) Production of Hydrated Metal Ions by Fast Ion or Atom Beam Sputtering. Collision-Induced Dissociation and Successive Hydration Energies of Gaseous Cu^+ with 1-4 Water Molecules. J Am Chem Soc 111:5036–5043. doi:10.1021/ja00196a003
112. Boryak OA, Stepanov IO, Kosevich MV, Shelkovsky VS, Orlov VV, Blagoy YP (1996) Origin of Clusters. I. Correlation of Low Temperature Fast Atom Bombardment Mass Spectra with the Phase Diagram of NaCl-Water Solutions. Eur Mass Spectrom 2:329–339. doi:10.1255/ejms.43
113. Kosevich MV, Boryak OA, Stepanov IO, Shelkovsky VS (1997) Origin of Clusters. II. Distinction of Two Different Processes of Formation of Mixed Metal/Water Clusters Under Low-Temperature Fast Atom Bombardment. Eur Mass Spectrom 3:11–17. doi:10.1255/ejms.28
114. Boryak OA, Kosevich MV, Shelkovsky VS, Blagoy YP (1996) Study of Frozen Solutions of Nucleic Acid Nitrogen Bases by Means of Low Temperature Fast-Atom-Bombardment Mass Spectrometry. Rapid Commun Mass Spectrom 10:197–199. doi:10.1002/(SICI)1097-0231(19960131)10:2<197::AID-RCM457>3.0.CO;2-G
115. Huang M-W, Chei HL, Huang JP, Shiea J (1999) Application of Organic Solvents As Matrixes to Detect Air-Sensitive and Less Polar Compounds Using Low-Temperature Secondary Ion Mass Spectrometry. Anal Chem 71:2901–2907. doi:10.1021/ac980516p
116. Hofmann P, Volland MAO, Hansen SM, Eisenträger F, Gross JH, Stengel K (2000) Isolation and Characterization of a Monomeric, Solvent Coordinated Ruthenium(II) Carbene Cation

Relevant to Olefin Metathesis. J Organomet Chem 606:88–92. doi:10.1016/S0022-328X(00)00288-6
117. Wang CH, Huang MW, Lee CY, Chei HL, Huang JP, Shiea J (1998) Detection of a Thermally Unstable Intermediate in the Wittig Reaction Using Low-Temperature Liquid Secondary Ion and Atmospheric Pressure Ionization Mass Spectrometry. J Am Soc Mass Spectrom 9:1168–1174. doi:10.1016/S1044-0305(98)00089-0
118. Giesa S, Gross JH, Hull WE, Lebedkin S, Gromov A, Krätschmer W, Gleiter R (1999) $C_{120}OS$: The First Sulfur-Containing Dimeric [60]Fullerene Derivative. Chem Commun:465–466. doi:10.1039/a809831j
119. Gross JH (1998) Use of Protic and Aprotic Solvents of High Volatility As Matrixes in Analytical Low-Temperature Fast-Atom Bombardment Mass Spectrometry. Rapid Commun Mass Spectrom 12:1833–1838. doi:10.1002/(SICI)1097-0231(19981215)12:23<1833::AID-RCM401>3.0.CO;2-O
120. König WA, Aydin M, Schulze U, Rapp U, Höhn M, Pesch R, Kalikhevitch VN (1983) Fast-Atom-Bombardment for Peptide Sequencing – A Comparison with Conventional Ionization Techniques. Int J Mass Spectrom Ion Phys 46:403–406. doi:10.1016/0020-7381(83)80137-5
121. Caprioli RM (1987) Enzymes and Mass Spectrometry: A Dynamic Combination. Mass Spectrom Rev 6:237–287. doi:10.1002/mas.1280060202
122. Caprioli RM (1988) Analysis of Biochemical Reactions with Molecular Specificity Using Fast Atom Bombardment Mass Spectrometry. Biochemistry 27:513–521. doi:10.1021/bi00402a001
123. Chait BT, Wang R, Beavis RC, Kent SB (1993) Protein Ladder Sequencing. Science 262:89–92. doi:10.1126/science.8211132
124. Naylor S, Findeis AF, Gibson BW, Williams DH (1985) An Approach Towards the Complete FAB Analysis of Enzymic Digests of Peptides and Proteins. J Am Chem Soc 108:6359–6363. doi:10.1021/ja00280a037
125. Deterding LJ, Tomer KB, Wellemans JMY, Cerny RL, Gross ML (1999) Capillary Electrophoresis/Tandem Mass Spectrometry with Array Detection. Eur Mass Spectrom 5:33–40. doi:10.1255/ejms.247
126. Lehmann WD (1996) Massenspektrometrie in der Biochemie. Spektrum Akademischer Verlag, Heidelberg
127. Chapman JR (ed) (2000) Mass Spectrometry of Proteins and Peptides. Humana Press, Totowa
128. Snyder AP (2000) Interpreting Protein Mass Spectra. Oxford University Press, New York
129. Kinter M, Sherman NE (2000) Protein Sequencing and Identification Using Tandem Mass Spectrometry. Wiley, Chichester
130. Stults JT, Lai J, McCune S, Wetzel R (1993) Simplification of High-Energy Collision Spectra of Peptides by Amino-Terminal Derivatization. Anal Chem 65:1703–1708. doi:10.1021/ac00061a012
131. Bordaz-Nagy J, Despeyroux D, Jennings KR, Gaskell SJ (1992) Experimental Aspects of the Collision-Induced Decomposition of Ions in a Four-Sector Tandem Mass Spectrometer. Org Mass Spectrom 27:406–415. doi:10.1002/oms.1210270410
132. Karlsson NG, Karlsson H, Hansson GC (1996) Sulfated Mucin Oligosaccharides from Porcine Small Intestine Analyzed by Four-Sector Tandem Mass Spectrometry. J Mass Spectrom 31:560–572. doi:10.1002/(SICI)1096-9888(199605)31:5<560::AID-JMS331>3.0.CO;2-0
133. Caprioli RM, Beckner CF, Smith LA (1983) Performance of a Fast-Atom Bombardment Source on a Quadrupole Mass Spectrometer. Biomed Mass Spectrom 10:94–97. doi:10.1002/bms.1200100209
134. Cornett DS, Lee TD, Mahoney JF (1994) Matrix-Free Desorption of Biomolecules Using Massive Cluster Impact. Rapid Commun Mass Spectrom 8:996–1000. doi:10.1002/rcm.1290081218

135. Mahoney JF, Perel J, Lee TD, Martino PA, Williams P (1992) Shock Wave Model for Sputtering Biomolecules Using Massive Cluster Impact. J Am Soc Mass Spectrom 3:311–317. doi:10.1016/1044-0305(92)87058-7
136. Mahoney JF, Cornett DS, Lee TD (1994) Formation of Multiply Charged Ions from Large Molecules Using Massive-Cluster Impact. Rapid Commun Mass Spectrom 8:403–406. doi:10.1002/rcm.1290080513
137. Sundqvist B, Macfarlane RD (1985) Californium-252-Plasma Desorption Mass Spectrometry. Mass Spectrom Rev 4:421–460. doi:10.1002/mas.1280040403
138. Macfarlane RD (1993) Californium-252-Plasma Desorption Mass Spectrometry I – A Historical Perspective. Biol Mass Spectrom 22:677–680. doi:10.1002/bms.1200221202
139. Macfarlane RD, Hu ZH, Song S, Pittenauer E, Schmid ER, Allmaier G, Metzger JO, Tuszynski W (1994) ^{252}Cf-Plasma Desorption Mass Spectrometry II – A Perspective of New Directions. Biol Mass Spectrom 23:117–130. doi:10.1002/bms.1200230302
140. Håkansson P, Kamensky I, Sundqvist B, Fohlman J, Peterson P, McNeal CJ, Macfarlane RD (1982) Iodine-127-Plasma Desorption Mass Spectrometry of Insulin. J Am Chem Soc 104:2948–2949. doi:10.1021/ja00374a053
141. Macfarlane RD (1999) Mass Spectrometry of Biomolecules: from PDMS to MALDI. Brazilian J Phys 29:415–421. doi:10.1590/S0103-97331999000300003
142. Sundqvist B, Håkansson P, Kamensky I, Kjellberg J (1983) Fast heavy ion induced desorption of molecular ions from small proteins. In: Benninghoven A (ed) Ion Formation from Organic Solids. Springer, Heidelberg
143. Macfarlane RD (1981) ^{252}Californium Plasma Desorption Mass Spectrometry. Biomed Mass Spectrom 8:449–453. doi:10.1002/bms.1200080918
144. Wien K, Becker O (1983) Secondary ion emission from metals under fission fragment bombardment. In: Benninghoven A (ed) Ion Formation from Organic Solids. Springer, Heidelberg
145. Zubarev RA, Abeywarna UK, Demirev P, Eriksson J, Papaléo R, Håkansson P, Sundqvist BUR (1997) Delayed, Gas-Phase Ion Formation in Plasma Desorption Mass Spectrometry. Rapid Commun Mass Spectrom 11:963–972. doi:10.1002/(SICI)1097-0231(19970615)11:9<963::AID-RCM878>3.0.CO;2-%23
146. Jonsson GP, Hedin AB, Håkansson P, Sundqvist BUR, Säve BGS, Nielsen P, Roepstorff P, Johansson KE, Kamensky I, Lindberg MSL (1986) Plasma Desorption Mass Spectrometry of Peptides and Proteins Adsorbed on Nitrocellulose. Anal Chem 58:1084–1087. doi:10.1021/ac00297a023
147. Wolf B, Macfarlane RD (1991) Small Molecules as Substrates for Adsorption/Desorption in Californium-252 Plasma Desorption Mass Spectrometry. J Am Soc Mass Spectrom 2:29–32. doi:10.1016/1044-0305(91)80058-F
148. Song S, Macfarlane RD (2002) PDMS-Chemistry of Angiotensin II and Insulin in Glucose Glass Thin Films. Anal Bioanal Chem 373:647–655. doi:10.1007/s00216-002-1361-4